

Perspectives from research on metal-semiconductor contacts: Examples from Ga_2O_3 , SiC, (nano)diamond, and SnS

Lisa M. Porter^{1,a)} and Jenifer R. Hajzus^{1,2)}

¹⁾Department of Materials Science and Engineering, Carnegie Mellon University, Pittsburgh, PA 15213

²⁾American Society for Engineering Education, Washington, DC 20036, USA

^{a)}Electronic mail: lporter@andrew.cmu.edu

As part of a Special Issue in Honor of 30 Years of the American Vacuum Society's Nellie Yeoh Whetten Award, this Invited Perspective discusses results and trends from the authors' and other published research on metal contacts to $\beta\text{-Ga}_2\text{O}_3$, (4H and 6H)-SiC, nanocrystalline diamond (NCD), and nanocrystalline thin films and single-crystalline nanoribbons of $\alpha\text{-SnS}$. The paper is not a comprehensive review of research on contacts to each of these semiconductors; it is instead a perspective that focuses on Schottky barrier height (Φ_b) measurements and factors that affect Φ_b , such as the metal work function (Φ_m) and crystallographic surface plane. Metals and the associated processing conditions that form ohmic or Schottky contacts to each of these semiconductors are also described. Estimates of the index of interface behavior, S , which measures the dependence of Φ_b on Φ_m , show large variations both among different semiconductors (e.g., $S \sim 0.3$ for NCD and $S \sim 1.0$ for SnS nanoribbons) and between different surface planes of the same semiconductor (e.g., $(\bar{2}01)$ vs. (100) Ga_2O_3). The results indicate that Φ_b is strongly affected by the nature of the semiconductor surface and near-surface region

and suggest that the sharp distinction between covalent and ionic semiconductors as described in seminal theories can be adjustable.

I. INTRODUCTION

Metal-semiconductor contacts serve as active or passive components in all semiconductor electronic devices such as diodes and field-effect transistors (FETs). Electrical, chemical, morphological, and other properties at metal-semiconductor interfaces often control or limit overall device performance. Therefore it is vital to understand how to control the properties of metal-semiconductor contacts, especially at device operating conditions.

The Schottky barrier height (Φ_b) represents the energy barrier to charge transport across a metal-semiconductor contact and is a key parameter that determines the electrical behavior of both ohmic and rectifying (a.k.a. Schottky) contacts. For ohmic contacts Φ_b affects the contact resistance, whereas Φ_b for Schottky contacts affects the turn-on voltage, reverse leakage current and other performance metrics. Because of the importance of Φ_b on the electrical properties of metal-semiconductor contacts, an inordinate amount of research has been devoted to measuring Φ_b for different metal-semiconductor contacts and to determining the materials and processing methods that enable its optimization for specific device applications. This Invited Perspective focuses on trends we've observed from our research on Schottky barrier heights of metal-semiconductor contacts, using four different semiconductors as examples: β -Ga₂O₃, (4H and 6H)-SiC, nanocrystalline diamond, and α -SnS. [Although not a comprehensive review, in this paper we attempt to put research results on \$\Phi_b\$ for the above semiconductors in context.](#)

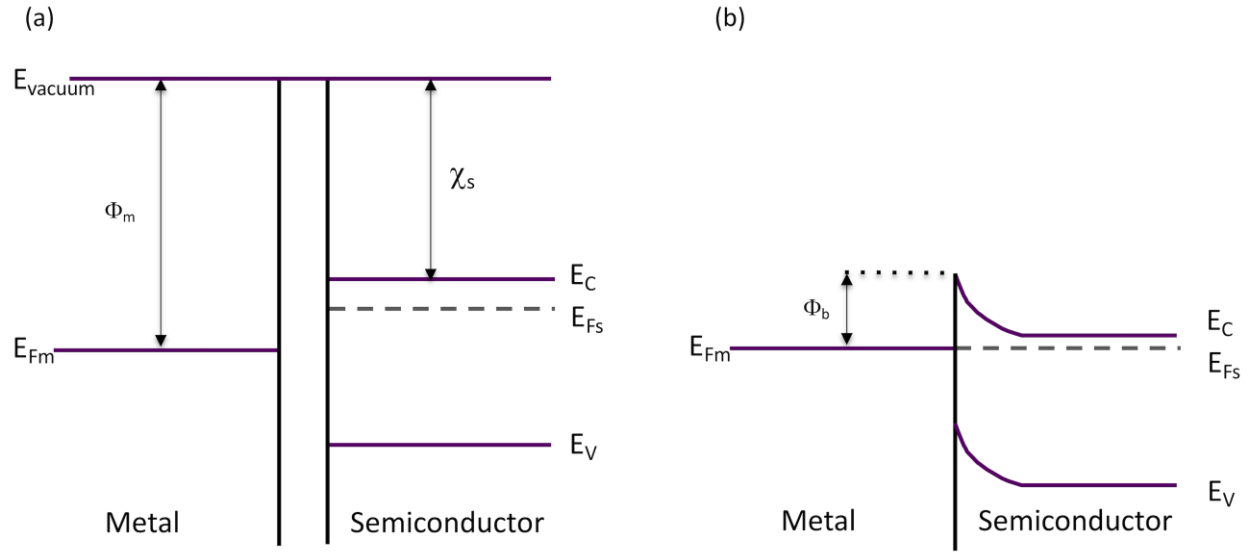


FIG. 1 . Electron energy band diagrams of a metal and n-type semiconductor (a) before and (b) after contact.

The formation of a Schottky barrier can be understood by referring to the electron energy diagrams of a typical metal and an n-type semiconductor (Fig. 1a). When the metal and semiconductor contact each other, the Fermi levels in each material align as a result of electron transport from the semiconductor to the metal, resulting in an upward band bending at the semiconductor surface (Fig. 1b). The Schottky-Mott relationship¹ follows from this described charge transport:

$$\Phi_b = \Phi_m - \chi_s, \quad (\text{Eqn. 1})$$

where Φ_m is the metal work function and χ_s is the electron affinity of the semiconductor. This ideal relationship therefore predicts that one can control Φ_b by choosing a metal with a proper Φ_m .

However, because of surface states², metal-induced gap states^{3,4}, or other factors, it is often found that Φ_b is either independent of or weakly dependent on Φ_m . The measure of correlation between Φ_b and Φ_m is called the index of interface behavior:

$$S = d\Phi_b/d\Phi_m. \quad (\text{Eqn. 2})$$

Kurtin, McGill and Mead⁵ reported a theoretical prediction, supported by (published and unpublished) experimental evidence, that highly covalently-bonded, inorganic semiconductors tend toward high densities of surface states, which leads to Φ_b 's that are independent of Φ_m (a.k.a. Fermi level pinning). In contrast, highly ionically-bonded semiconductors are expected to have low densities of surface states and therefore close correspondence with the Schottky-Mott relationship (Eqn. 1). In the sections that follow, we provide examples from published results of Φ_b 's on four different semiconductors with different degrees of covalent/ionic bonding. We discuss observed trends and our interpretations of how the results coincide with the seminal theories.

II. Ga₂O₃

Gallium oxide is an ultra-wide bandgap semiconductor that exists in a number of different polymorphs.⁶ β -Ga₂O₃ ($E_g \sim 4.8$ eV) is the stable polymorph at atmospheric pressure at all temperatures up to its melting point;⁷ this monoclinic polymorph is also the phase that grows from the melt and is the one most studied. The availability of commercially-grown, single-crystal β -Ga₂O₃ substrates, along with the high figure-of-merit for power devices⁸ and wide range of n-type doping (no p-type doping), have made Ga₂O₃ a highly promising semiconductor technology for ultra-high efficiency electronics. Although various Ga₂O₃ polymorphs have been grown heteroepitaxially on sapphire and other substrates,⁹ less research has been conducted on the metastable Ga₂O₃ phases. The perspective given in this section focuses exclusively on Schottky and ohmic contacts to β -Ga₂O₃. [For Schottky contacts, we focus here on studies that included multiple metals within the same study. To see a more comprehensive review of studies on individual](#)

Schottky metal contacts to (100), (010), ($\bar{2}01$), and (001) Ga₂O₃ surfaces, the reader is referred to Lyle et al.¹⁰

Ga₂O₃ has been reported to have an upward band bending at the surface,¹¹⁻¹³ unlike some other n-type transparent conducting oxides such as In₂O₃.¹⁴ Because of this upward band bending, Schottky contacts tend to form naturally on Ga₂O₃. However, research to date indicates that properties of the contacts, such as the Schottky barrier heights, are dependent upon the particular Ga₂O₃ surface on which the contacts are deposited.

Schottky contacts also tend to be dependent on the surface preparation. Prior to contact deposition, Ga₂O₃ substrates have typically been cleaned with organic solvents and one or more of the following wet chemicals: buffered oxide etch (BOE), HF, H₂SO₄, H₂O₂, HCl.¹⁵⁻¹⁷

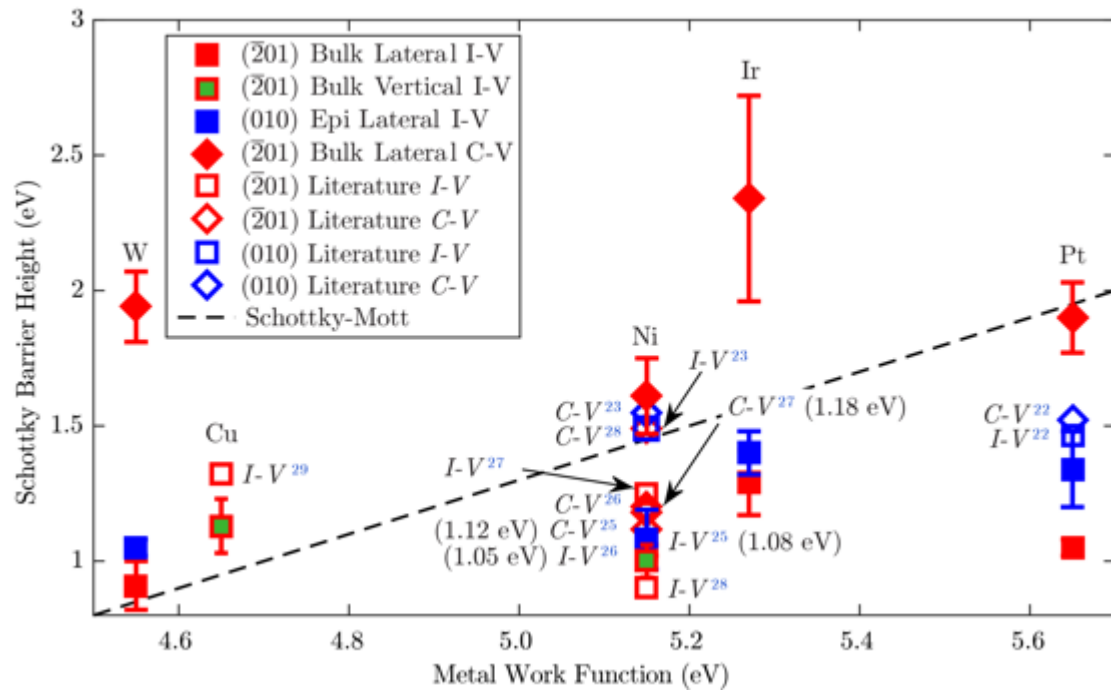


FIG. 2. Calculated Schottky barrier heights vs. metal work function for Schottky diodes on ($\bar{2}01$) bulk and epitaxial β -Ga₂O₃. Schottky barrier height values on ($\bar{2}01$) Ga₂O₃ as

reported in the literature are also included for comparison. Reprinted with permission from Y. Yao, *et al.*, *J. Vac. Sci. Technol. B* **35**, 03D113 (2017). Copyright 2017, American Vacuum Society.

We found that Schottky barrier heights of W, Cu, Ni, Ir, and Pt contacts on the ($\bar{2}01$) surface of β -Ga₂O₃ showed little dependence on the metal work function ¹⁷ (Fig. 2). The results indicate significant Fermi level pinning for Schottky contacts to ($\bar{2}01$) Ga₂O₃. This result was attributed to near-surface defects and/or unpassivated surface states.

In a different study by Hou *et al.*,¹¹ Schottky contacts of metal-oxides were reported to have higher Φ_b 's and better thermal stability on ($\bar{2}01$) β -Ga₂O₃ than their unoxidized metal counterparts (Fig. 3). These results also show a narrow range (1.3-1.4 eV) of Φ_b 's for the pure unoxidized metals, suggesting significant Fermi level pinning, which concurs with the results of Yao *et al.*¹⁷ for contacts on ($\bar{2}01$) β -Ga₂O₃.

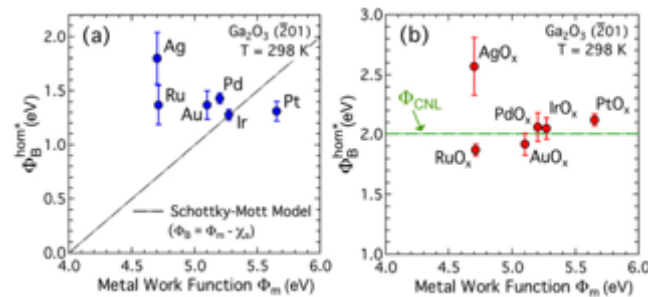


FIG. 3. Image-force-corrected laterally homogeneous barrier height (Φ_B^{hom}) versus metal work function (Φ_m) for (a) plain metal and (b) oxidized metal Schottky contacts on β -Ga₂O₃. Reprinted from C. Hou, *et al.*, *Appl. Phys. Lett.* **114**, 033502 (2019), with the permission of AIP Publishing.

In contrast, Farzana et al. reported a correlation between the Schottky barrier height and metal work function for three out of four metals (Pd, Ni, Pt) on (010) β -Ga₂O₃ (Fig. 4).¹⁸ Interestingly, Au was an outlier that displayed anomalous behavior associated with possible Fermi level pinning. Recent work in our group on (100) β -Ga₂O₃¹⁹ also suggests that metal work function has a significant effect on the Schottky barrier heights on this Ga₂O₃ surface.

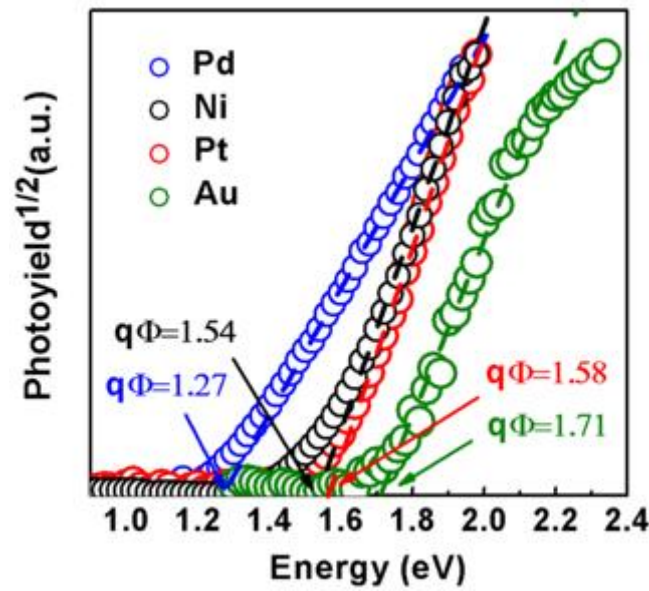


FIG. 4. Internal photoemission results for UID (010) β -Ga₂O₃ Schottky diodes at 300 K. Dashed lines are linear fits to determine the extracted Schottky barrier height values Reprinted from E. Farzana, *et al.*, *Appl. Phys. Lett.* **110**, 202102 (2017), with the permission of AIP Publishing.

Hou et al.¹¹ propose that stronger Fermi level pinning on the ($\bar{2}01$) surface may be associated with its higher oxygen dangling bond density and to the presence of oxygen vacancies – specifically the V_O(III) defect, which is believed to have a transition level 1.3 eV below the conduction band. Although the oxidized metals had higher barrier heights

than their unoxidized counterparts, the Φ_b 's of the oxidized metals also did not show much correlation with metal work function.

While many metals form Schottky contacts to Ga_2O_3 , only a few metals have proven the ability to form ohmic contacts. Although one might predict that low work function metals should form ohmic contacts to Ga_2O_3 , we investigated nine different low-to-moderate work function metals and found that most did not form ohmic contacts even after annealing at temperatures up to 600–800 °C.²⁰ The results of the study showed that morphology can be a substantial problem: a number of metals dewet the surface either before or after annealing, especially those that have low chemical affinity with Ga_2O_3 . Interfacial reactions appear to play an important role in ohmic contact formation; a limited amount of reaction at the interface between the metal and Ga_2O_3 can promote ohmic behavior, whereas too much results in degradation of the contacts. [The problem with forming ohmic contacts to \$\text{Ga}_2\text{O}_3\$ may also be associated with reaction-driven defects states that are too deep within the wide band gap to be effective donor sites, which is in contrast with defect-assisted ohmic contact formation in other semiconductors such as \$\text{ZnO}\$.](#)^{21, 22}

This is the author's peer reviewed, accepted manuscript. However, the online version of record will be different from this version once it has been copyedited and typeset.
PLEASE CITE THIS ARTICLE AS DOI: 10.1116/1.5144502

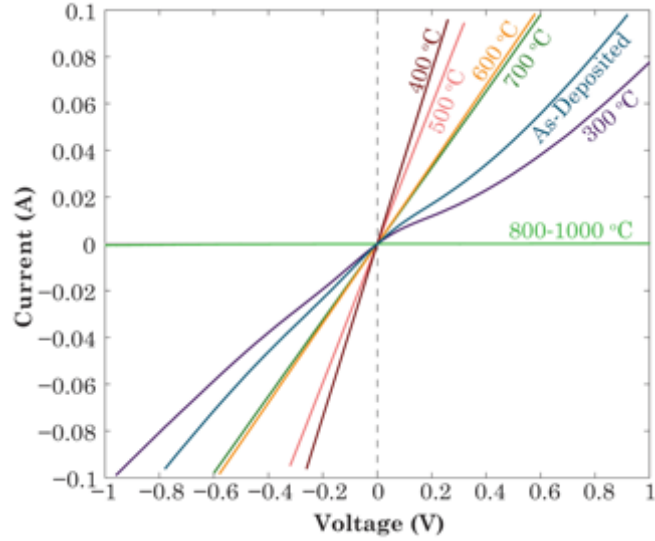


FIG. 5. I-V plots of Ti/Au on Sn-doped ($\bar{2}01$) β -Ga₂O₃ after annealing at the indicated temperatures in argon for 1 min. Reprinted by permission from Springer Nature: *Journal of Electronic Materials* (<https://www.springer.com/journal/11664>), Y. Yao, *et al.*, *Electron. Mater.* **46**, 2053 (2016), Copyright 2016.

Titanium, which is widely used as an ohmic contact to Ga₂O₃, exemplifies the role that interfacial reaction plays in ohmic contact formation. Our annealing study of Ti/Au (20 nm / 100 nm) contacts on Sn-doped ($\bar{2}01$) Ga₂O₃ (Fig. 5) showed that the resistivity is minimized after annealing at 400–500 °C for 1 min. Because Ti has a stronger thermodynamic driving force for oxidation than Ga, annealing causes Ti to reduce Ga₂O₃ to form Ti-oxide. Titanium oxide formation and significant interdiffusion of the Ti and Au layers were evidenced in cross-section TEM and EDX profiles after annealing at 400 °C for 1 min.²⁰ A high-resolution TEM study²³ confirmed that an ~5 nm TiO_x layer forms at the interface of Ti/Au contacts on Ga₂O₃ after annealing at 470 °C for 1 min. in N₂ (Fig. 6a). It was hypothesized that the ohmic behavior is due in part to the formation of a thin TiO_x layer with a relatively small bandgap and the indiffusion of Au to form a

low resistivity layer (Fig. 6b). A specific contact resistivity value of $4.6 \times 10^{-6} \Omega \text{ cm}^2$ was achieved for Ti/Au contacts in Ga_2O_3 depletion-mode MOSFETs by Si^+ implantation at room temperature, followed by a 950°C post-implant anneal.²⁴

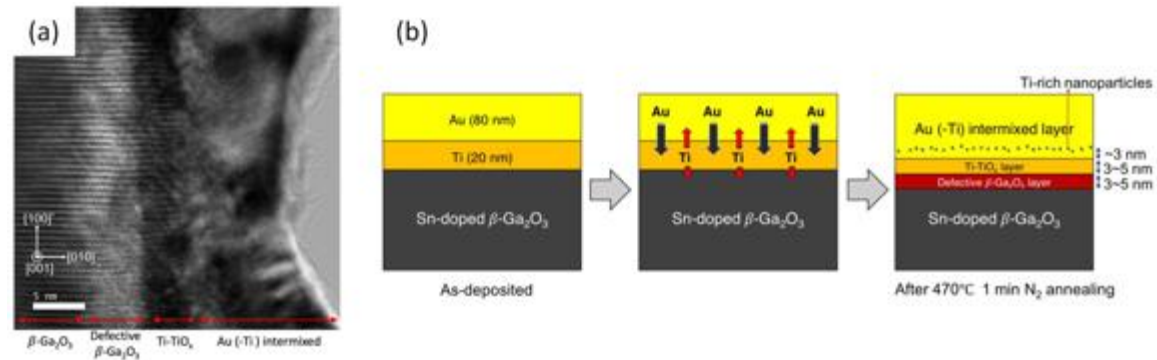


FIG. 6. (a) HRTEM image of Ti/ β - Ga_2O_3 after annealing at 470°C for 1 min. in N_2 , and (b) schematic diagrams of the evolution of Ti/Au contacts during the anneal process. M.-H. Lee and R. L. Peterson, *APL Mater.* **7**, 022524 (2019); licensed under a Creative Commons Attribution (CC BY) license. Copyright 2019, M.-H. Lee and R. L. Peterson.

Although the reactivity between Ti and Ga_2O_3 appears to be beneficial to forming an ohmic contact, the reaction is not self-limiting. Annealing for longer times at the same temperature or at higher temperatures should increase the thickness of Ti-oxide. The degradation in the electrical behavior of Ti/Au contacts annealed at $T > 500^\circ\text{C}$ is attributed to the formation of a thicker TiO_x non-conductive/low-conductivity layer. For stable operation of Ga_2O_3 devices at elevated temperatures over extended time periods, it will be important to develop contact metallization schemes that are both electrically and thermally stable.

A recent study reports that Mg/Au (820 nm / 600 nm) contacts on Sn-doped ($\bar{2}01$) β - Ga_2O_3 were ohmic after annealing for 2 min. in Ar at temperatures between 300 and 500°C .²⁵ A minimum contact resistance of $2.1 \times 10^{-5} \Omega \text{ cm}^2$ on the $4 \times 10^{17} \text{ cm}^{-3}$

substrate was calculated after a 500 °C anneal. It is perhaps encouraging that this additional metallization scheme has demonstrated ohmic behavior on Ga₂O₃. However, a caveat is that Mg has an even higher driving force for oxidation than Ti and therefore is also unstable on Ga₂O₃. The authors of the study found that the electrical characteristics degraded when annealed at 600 °C.

In summary, metal contacts to Ga₂O₃ tend to form Schottky contacts in the as-deposited condition, a result attributed in part to the reported upward band bending at the Ga₂O₃ surface. Reports in the literature indicate that the properties and behavior of Schottky contacts depend on the particular Ga₂O₃ surface on which the contacts are deposited. A few studies, discussed in this section, have each reported electrical measurements of four or more metals on ($\bar{2}01$), (010), and (100) Ga₂O₃ surfaces, respectively. The results suggest that Schottky barrier heights on the ($\bar{2}01$) surface are dominated by Fermi level pinning, which has been attributed to the presence of specific defects and a high dangling bond density. Schottky barrier heights for a limited number of metals on the (010) and (100) surfaces have generally shown a correlation with the metal work functions, although typically less than that predicted by the Schottky-Mott theory. The data also suggest that Schottky barrier heights tend to be higher on (010) than on ($\bar{2}01$) or (100) surfaces. The reasons for these differences are still under investigation. Notably, fewer metals have been demonstrated as ohmic contacts to Ga₂O₃. Ti/Au contacts annealed at 400–500 °C are widely used, and techniques such as Si⁺ implantation have been employed successfully to achieve specific contact resistances in the 10⁻⁶ Ω cm² range.²⁴ However, the instability of the Ti/Ga₂O₃ interface indicates

that contact metal schemes with enhanced stability will be needed for long-term device operation at elevated temperatures.

III. SiC

Silicon carbide (4H-SiC) is being increasingly used as a semiconductor platform in commercial high power devices and is expected to continue to replace silicon in a broad range of high power applications, for which reliability testing of the SiC devices is an ongoing concern of paramount importance.²⁶ Commercial devices include 1-kV Schottky barrier diodes and vertical power MOSFETs.²⁷ 3C-SiC is of interest because of its higher electron mobility, and 3C-SiC MOSFETs with significantly higher channel mobility than 4H-SiC MOSFETs have been demonstrated. However, 3C-SiC is plagued by much higher defect densities, and there are currently no large area seed crystals of this polytype, although people are working on fabricating them via a growth and transfer process.²⁸

Our early metal contact studies on SiC were conducted mostly on (0001) 6H-SiC. The nature of the semiconductor surface prior to metal contact deposition is critically important for determining the behavior of metal-semiconductor contacts, especially for covalently bonded semiconductors like SiC. We developed a chemical and thermal cleaning process,²⁹ which consisted of oxidizing the surface to remove excess C (present on as-received epitaxial films), etching in a 10% HF aqueous solution to remove the oxide layer, and heating in ultra-high vacuum at 700 °C to remove hydrocarbons from the surface. This temperature was chosen to prevent graphitization of the SiC surface, which can begin to occur at 800 °C in vacuum.³⁰ It's important to note that characterization using XPS showed residual O and a trace amount of F were still present on the SiC

surface after this chemical and heat treatment. (Note that it has proven very difficult to produce a perfectly clean, undamaged, atomically ordered SiC surface without employing complex methods, such as high temperature annealing with a simultaneous controlled flux of a vapor species like Si or H₂.) XPS characterization also revealed an upward band bending at the surface of a few tenths of an eV, indicating the presence of surface states.

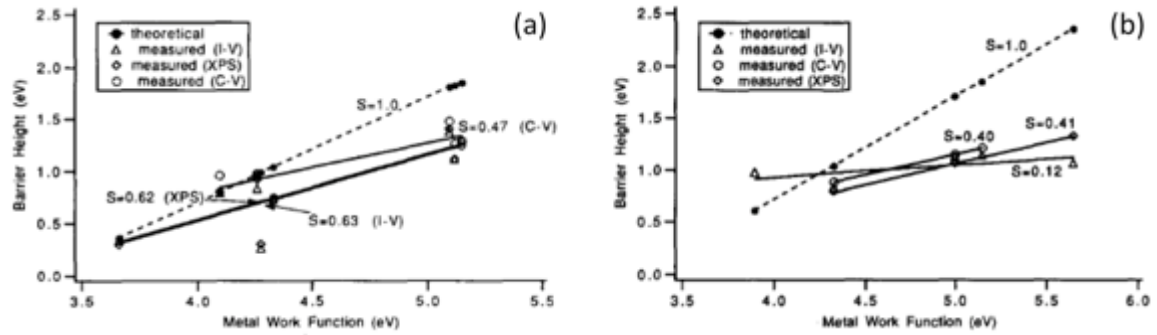


FIG. 7. Data points of experimentally-determined and theoretical barrier heights on n-type 6H-SiC (0001) vs. metal work function. The experimental data points are from (a) Waldrop *et al.*^{31, 32} and (b) Porter *et al.*^{29, 33-35} The slopes, S , of the linear fits through each set of data points are shown. Reprinted from *Materials Science and Engineering: B*, vol. 34, L. M. Porter and R. F. Davis, “A critical review of ohmic and rectifying contacts for silicon carbide,” pp. 83-105, Copyright 1995, with permission from Elsevier.

Deposition of metals in ultra-high vacuum onto n-type 6H-SiC surfaces treated using the above process tended to yield excellent Schottky contacts, as characterized by low (near 1.0) ideality factors and low leakage currents³³. Investigation of several different metal contacts by Porter *et al.*^{29, 33, 34, 36} and Waldrop *et al.*^{31, 32} show positive correlations between the metal work functions and Φ_b 's as calculated from XPS, I-V and C-V measurements (Fig. 7). Interestingly, Φ_b 's on the C-terminated (000 $\bar{1}$) surface tend to be higher than those on the Si-terminated (0001) surface.

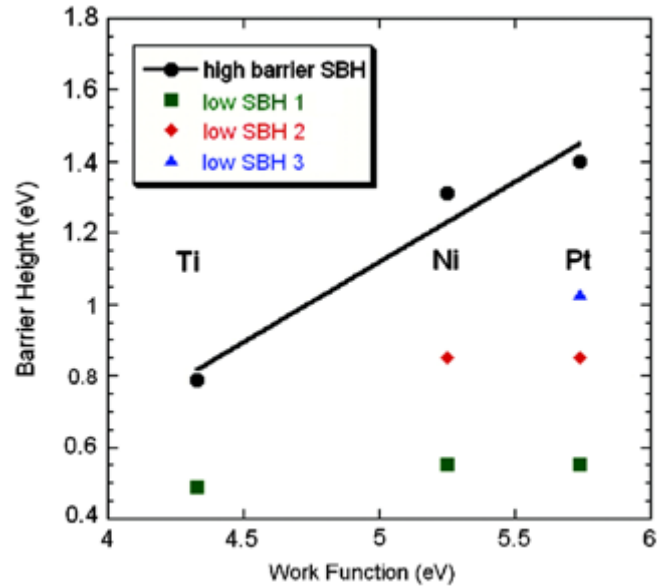


FIG. 8. Schottky barrier heights for high and low Schottky barriers to commercial 4H-SiC vs. metal work function. The line, with slope $S = 0.45$, is a fit to the barrier heights for near-ideal diodes. Reprinted from D. J. Ewing, *et al.*, *J. Appl. Phys.* **101**, 114514 (2007), with the permission of AIP Publishing.

Metal contact studies on n-type (0001) 4H-SiC, [cleaned using the procedure described above](#), also indicate the ideal Schottky barrier height increases with metal work function ³⁷. The index of interface behavior (Eqn. 2) for Ti, Ni, and Pt contacts was estimated to be $S = 0.45$ (Fig. 8), which is similar to S values extracted for 6H-SiC. However, a significant fraction of diodes on 4H-SiC epilayers showed inhomogeneous behavior that was modeled as two (low and high) Schottky barriers in parallel (Fig. 9b). ³⁷⁻⁴⁰ Ewing et al.'s analysis of hundreds of diodes pointed to the low barriers clustering around three values (~ 0.60 , 0.85 , and 1.05 eV), which were independent of the metal

This is the author's peer reviewed, accepted manuscript. However, the online version of record will be different from this version once it has been copyedited and typeset.
PLEASE CITE THIS ARTICLE AS DOI: 10.1116/1.5144502

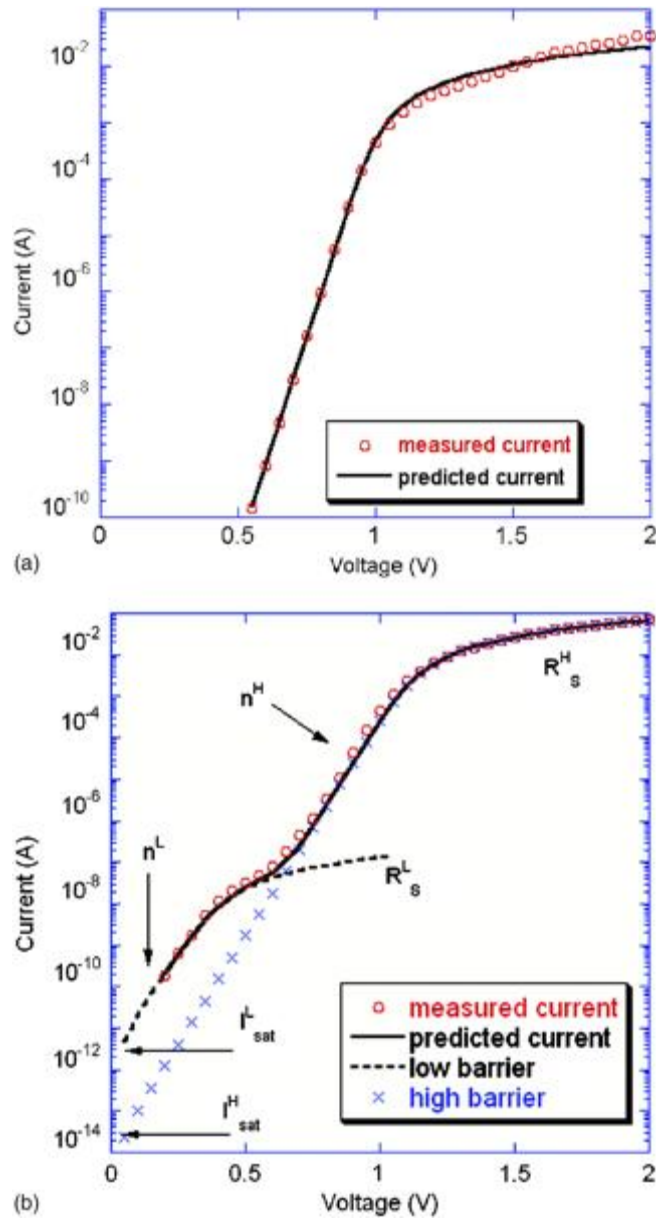


FIG. 9. (a) Single-barrier and (b) double-barrier Ni Schottky diodes on 4H-SiC with commercially grown epitaxial layers. Open circles denote the current measured experimentally, and the solid and dashed lines denote the current predicted by the models. Reprinted from D. J. Ewing, *et al.*, *J. Appl. Phys.* **101**, 114514 (2007), with the permission of AIP Publishing.

work function. By comparing electrical measurements with investigations using a variety of spectroscopic and imaging techniques, the low barriers were attributed to localized

This is the author's peer reviewed, accepted manuscript. However, the online version of record will be different from this version once it has been copyedited and typeset.
PLEASE CITE THIS ARTICLE AS DOI: 10.1116/1.5144502

Fermi level pinning by defects, such as 3C-SiC stacking faults, in the 4H-SiC epilayers.^{37, 38} In cases where the local concentration of defects within the diode area was high, both the work function and near-surface dipoles induced by subsurface defects contribute to Schottky barrier formation.²²

Ohmic contacts to SiC with low contact resistance are needed to keep device on-resistances low.⁴¹ Nickel is most commonly used as the ohmic contact to n-type SiC. Annealing at 900–1000 °C produces Ni₂Si and $\rho_c \sim 10^{-5}$ – 10^{-6} Ω cm². It is difficult to obtain ohmic contacts with low ρ_c to p-type SiC, primarily because of its large band gap and work function. It's interesting to note a prediction we made 25 years ago, that “the ability to create ohmic contacts with low contact resistivities ($\leq 10^{-6}$ Ω cm²) will be one of the major challenges facing the SiC community in the foreseeable future,”³³ has largely held true to this day. For p-type SiC, contacts containing Al (a p-type dopant in SiC) can be annealed to cause Al to diffuse into the SiC, yielding a high p-type concentration at the surface.^{33, 42} The high p-type concentration produces a narrow depletion region through which holes can tunnel. Ti/Al contacts annealed >800 °C can achieve ρ_c 's of 10^{-4} – 10^{-5} Ω cm² on p-type SiC. Roccaforte et al.⁴¹ point to the Ti/Al/Ni stack as being particularly promising as a stable p-type metallization scheme. A few groups⁴³⁻⁴⁵ worked on developing metallizations that simultaneously form thermally stable ohmic contacts to n-type and p-type 4H-SiC in order to simplify device fabrication processes and allow devices to operate at high temperatures. Zhang et al.⁴⁴ formed ohmic contacts on ion implanted n- and p-type SiC by annealing Pt/TaSi₂/Ni/Ti/Ni/SiC at 975 – 1100 °C. The contacts were still ohmic after heating at 500 °C for 300 h in air, and ρ_c values were relatively stable, as shown in Fig. 10.

This is the author's peer reviewed, accepted manuscript. However, the online version of record will be different from this version once it has been copyedited and typeset.
PLEASE CITE THIS ARTICLE AS DOI: 10.1116/1.5144502

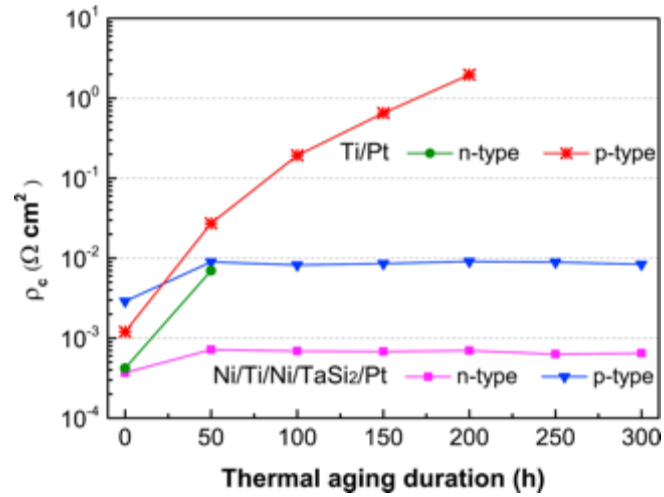


FIG. 10. Specific contact resistance as a function of thermal aging for Pt/TaSi₂/Ni/Ti/Ni/SiC samples. Reprinted from *Journal of Alloys and Compounds*, vol. 731, Y. Zhang, T. Guo, X. Tang, J. Yang, Y. He and Y. Zhang, “Thermal stability study of n-type and p-type ohmic contacts simultaneously formed on 4H-SiC,” pp. 1267-1274, Copyright 2018, with permission from Elsevier.

In summary, metal contacts to SiC are being employed in commercial high power devices. Past research by our group and others indicates that Schottky barriers form on SiC (6H or 4H) with an index of interface behavior, $S \sim 0.4$, following standard chemical cleaning procedures that likely leave minor (submonolayer) impurities on the SiC surface. Barrier height inhomogeneities associated with high local concentrations of specific defects have been identified in research labs and may be associated with device reliability issues. Annealed Ni and Al-containing contacts tend to be used to form ohmic contacts to n- and p-type SiC, respectively. Producing contacts with reduced contact resistance and enhanced thermal stability is an ongoing challenge to realize the full potential of SiC for extreme operating conditions.

IV. NANOCRYSTALLINE DIAMOND

Nanocrystalline diamond (NCD) is generally described as comprising crystalline grains (typically 10's of nanometers in size) and grain boundaries that contain predominantly sp^3 -bonded and sp^2 -bonded carbon atoms, respectively.⁴⁶ Conductivity in NCD films is ascribed to conduction within grain boundaries, probably through hopping and impurity band conduction.⁴⁷ The p-p* states, associated with sp^2 bonding in the grain boundaries, strongly affect the optical and electronic properties of NCD.⁴⁷ Preferential incorporation of impurities into the grain boundaries coincides with n-type (e.g., N or S) doping, whereas conventional doping with boron can lead to p-type conductivity in these films.⁴⁶ The broader control over the conductivity and carrier type in NCD is considered an advantage relative to conventional diamond films, although the small grain size yields low mobility values. Outside of optical coatings and various tribological and mechanical applications, NCD films are of interest for electrodes, sensors, field-emission devices, micro-electro-mechanical (MEMS) devices, etc.

Unintentionally-doped, n-type NCD films displayed evidence of a negative electron affinity and a (pseudo)bandgap of 5.0 ± 0.4 eV⁴⁸. In this same study we found that four metals (Zr, Ti, Cu and Pt), comprising a considerable range of work functions, formed ohmic contacts to n-type NCD films. Specific contact resistances increased with the metal work function for both undoped and S-doped films. Since ρ_c depended on Φ_b , the results suggest that the Schottky barrier height increased with increasing metal work function, in at least partial accordance with the Schottky-Mott theory (Eqn. 1). Contact resistance values on the S-doped films were approximately two orders of magnitude lower than for undoped films when comparing the same metal contacts.

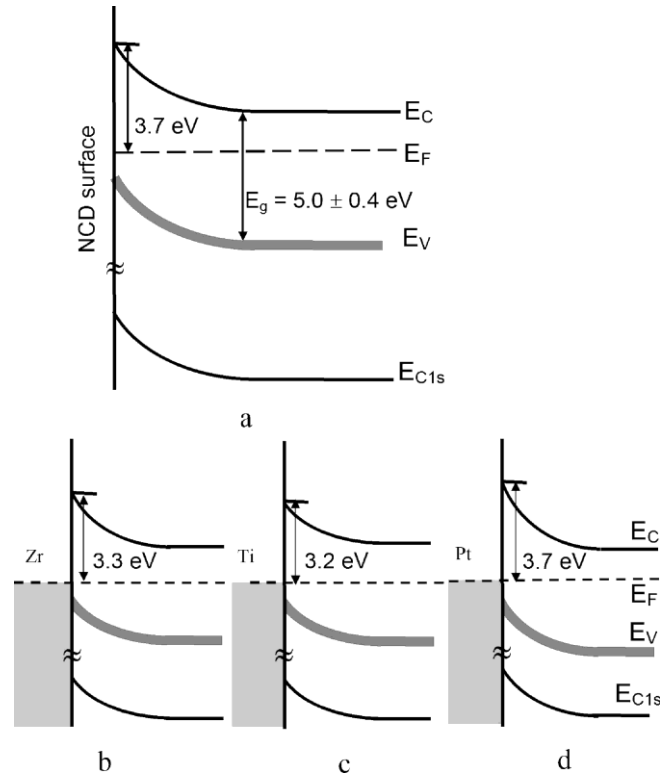


FIG. 11. Schematic of proposed band diagram for undoped NCD showing band gap (E_g), Fermi level (E_F), conduction band minimum (E_C), valence band maximum (E_V), and C 1s core-level (E_{C1s}) energies before (a) and after [(b)–(d)] Zr, Ti, and Pt deposition.

Reprinted from P. Kulkarni, *et al.*, *J. Appl. Phys.* **103**, 084905 (2008), with the permission of AIP publishing.

Photoemission measurements⁴⁸ of Zr, Ti, and Pt on NCD films confirmed that Φ_b for Pt (3.7 eV) is higher than the Φ_b 's for the low work function metals (3.3 eV for Zr and 3.2 eV for Ti) although the difference in Φ_b 's is only about 1/3 of the difference in their work function values (Fig. 11). Another conclusion from this study is that the ohmic behavior is likely due to carrier transport through low- Φ_b grain boundary regions. Due to the hopping and impurity band conduction in NCD films, it is plausible that trap-assisted tunneling is a parallel current transport mechanism at the metal-NCD interfaces.

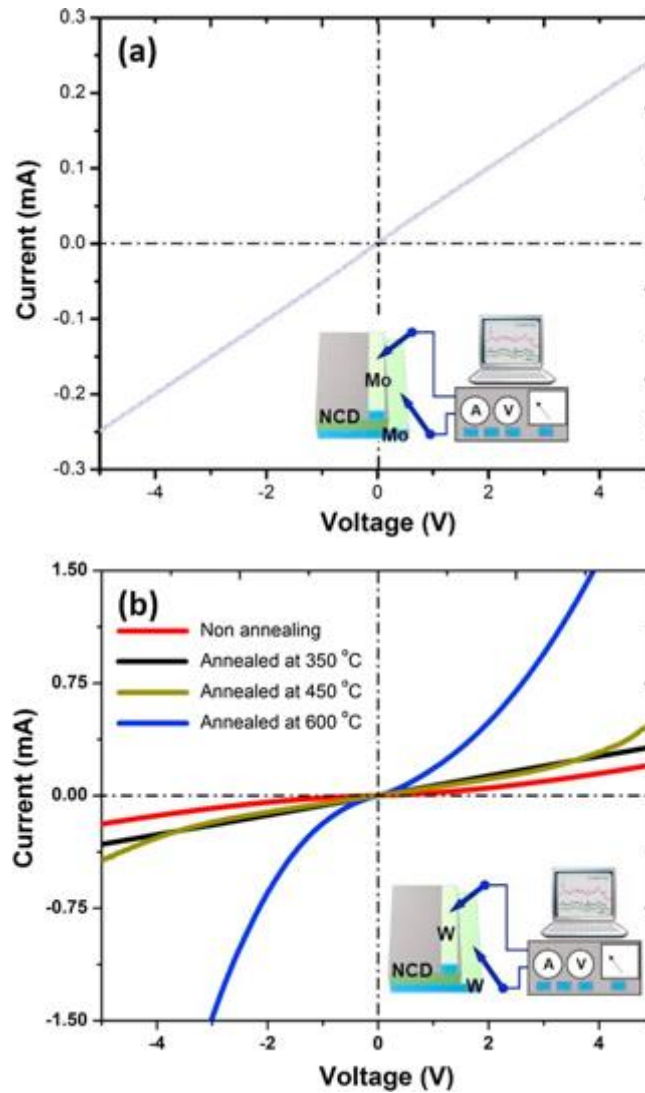


FIG. 12. I-V characteristics of (a) Mo/NCD/Mo and (b) W/NCD/W metal-semiconductor-metal UV photodetectors. Reprinted from *Applied Surface Science*, vol. 455, C.-W. Liu, J.-A. Lee, Y.-T. A. Sun, M.-K. BenDao and C.-R. Lin, “Effects of metallic interlayers on the performance of nanocrystalline diamond metal-semiconductor-metal photodetectors,” pp. 581-590, Copyright 2018, with permission from Elsevier.

Contacts to NCD films are generally reported to be ohmic (e.g., Ag⁴⁹; Ti and Cr⁵⁰; Au, Cr, Cu, Pt, and Ti⁵¹) even though the reported surface preparation methods vary greatly among the different studies: e.g., in-situ heating in ultra-high vacuum; exposure to H₂ plasma; or wet chemical cleaning in concentrated HCl. Vojs et al.⁵² found that the

contact resistance to NCD films depends on the annealing conditions, film thickness, and film morphology in addition to the particular metal. UV photodetectors based on NCD employed Au⁵³ or W⁵⁴ ohmic contacts. Fig. 12 shows I-V characteristics of metal-semiconductor-metal (MSM) NCD photodetectors using Mo and W, respectively. Both metals were ohmic in the as-deposited condition, but the W contacts were annealed up to 600 °C to reduce the contact resistance.

Tadjer et al.⁵⁵ also found that different metals (Al, Ti/Al, Ti/Au, and Ni/Au) formed ohmic contacts in the as-deposited condition to B-doped, p-type NCD films. It is interesting that the contact resistances were lower for the low-work function metals even though the films were p-type. The boron doping level had a much larger effect on lowering the contact resistance than did the particular metal.

One study reports that contacts changed from ohmic to “near Schottky” after hydrogen plasma treatment⁵⁶ of nitrogen-incorporated NCD. Au Schottky diodes to boron-doped NCD films with low-doped cap layers have also been reported⁵⁷.

In summary, most metal contacts on NCD (n-type, p-type, or unintentionally-doped) films are reported to be ohmic. The ohmic behavior of metals on NCD films is contrary to the typical Schottky behavior observed on conventional p-type diamond films, which require annealing or other processing steps to form ohmic contacts.⁵¹ Measurements of NCD films reported in the literature indicate that their electrical properties are largely governed by conduction within the nanocrystalline grain boundaries, which likely contributes to the different behavior of contacts to NCD vs. conventional diamond films. It is important to note, however, that even with grain boundary dominant conduction, the contact resistances to n-type and undoped NCD films

showed significant dependence on the metal work functions. This result, along with direct photoemission measurements, indicates that Schottky barrier heights to NCD films depend on the choice of metal. Contact resistances to both n-type (S-doped) and p-type (B-doped) NCD films also showed a strong dependence on the doping level, indicating that the electrical behavior can be controlled by different variables.

V. SnS

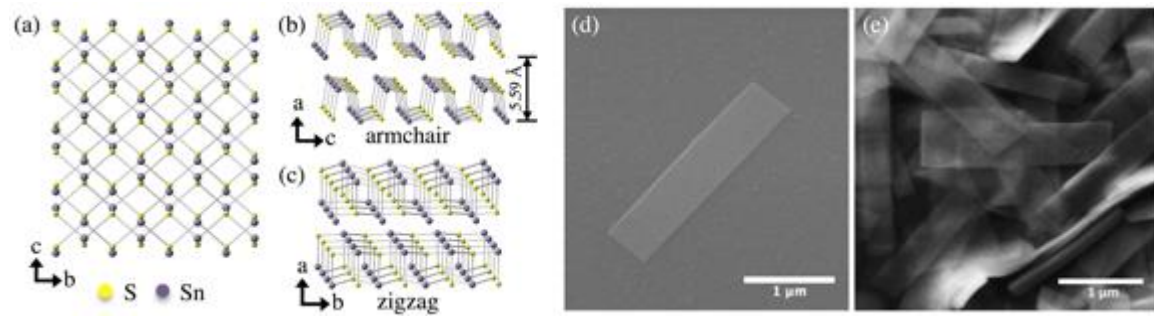


FIG. 13. Crystal structure of orthorhombic α -SnS viewing from the (a) (100) plane, and slightly tilted from the (b) (010), and (c) (001) planes. SEM images of (d) a single solution-synthesized SnS nanoribbon on a SiO₂/Si substrate and (e) a high concentration of SnS nanoribbons. J. R. Hajzus, A. J. Biacchi, S. T. Le, C. A. Richter, A. R. Hight Walker and L. M. Porter, *Nanoscale*, 2018, **10**, 319 - Reproduced by permission of The Royal Society of Chemistry.

Tin (II) sulfide is a natively p-type, moderate band gap semiconductor comprised of low-toxic, earth abundant elements and is most stable in the orthorhombic α -SnS polytype at standard conditions.^{58, 59} The favorable band gap ($E_g = \sim 1.1$ eV, indirect; ~ 1.3 eV, direct), high optical absorption coefficient ($> 10^5$ cm⁻¹ in the visible range), and undoped hole concentration ($10^{15} - 10^{18}$ cm⁻³) of α -SnS has motivated its study as a promising candidate for thin film solar cells.⁶⁰⁻⁶² SnS has also recently attracted attention for its high thermoelectric performance⁶³ and for applications in battery anode⁶⁴ and photodetector devices.⁶⁵ The crystal structure of α -SnS consists of two-atom thick,

buckled layers of strongly bonded Sn-S atoms separated by weaker interactions (Fig. 13 a-c).⁶⁶ α -SnS is an analogue of black phosphorous/phosphorene with lower symmetry due to the presence of two different elements.⁶⁷ Computational studies have predicted intriguing properties of two-dimensional SnS such as a thickness-tunable bandgap (~ 1.1 eV in bulk to ~ 2 eV in monolayer, indirect),^{62, 67-71} high piezoelectric coefficient,⁷² and ferroelectricity/ferroelasticity.⁷³ While two-dimensional SnS monolayers have yet to be produced by mechanical exfoliation, isolation of SnS monolayers and bilayers by liquid phase exfoliation^{74, 75} and post-thinning techniques⁷⁶ has been reported. The orthorhombic, layered structure of α -SnS gives rise to anisotropic optical and electrical properties^{77, 78} and orientation-dependent surface energies⁷⁹ and electron affinities.⁸⁰

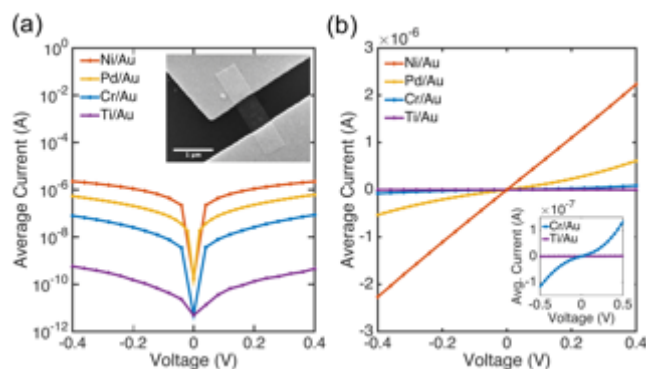


FIG. 14. Average I–V sweeps for different contact metallizations on SnS nanoribbons on a (a) log and (b) linear scale, showing ohmic and semi-ohmic behavior for Pd/Au and Ni/Au contacts, and back-to-back Schottky behavior for Cr/Au and Ti/Au contacts. Inset in (a) is an SEM image of two Ni/Au contacts on a SnS nanoribbon. Reprinted with permission from J. R. Hajzus, A. J. Biacchi, S. T. Le, C. A. Richter, A. R. Hight Walker and L. M. Porter, *Nanoscale*, 2018, **10**, 319 - Reproduced by permission of The Royal Society of Chemistry.

Contacts to the (100) surface of individual, solution synthesized, p-type α -SnS semiconductor nanocrystals (Fig. 13 d, e) showed ohmic or semi-ohmic behavior for high

work function metals (Ni and Pd) and rectifying behavior for lower work function metals (Cr and Ti) (Fig. 14 a, b).⁸¹ The behavior follows closely that predicted by Schottky-Mott theory (Fig. 15 a, b): specifically, the calculated Φ_b 's were 0.39 and 0.50 eV for Cr and Ti, respectively. Other discrete results in the literature (e.g., Ag⁸² and Ni⁸³) also fit this trend and suggest that Schottky-Mott behavior should prevail on single crystalline (100) SnS surfaces. Transfer length method (TLM) and contact end resistance test structures were fabricated using electron-beam lithography onto individual, SnS nanoribbons that were several μm long, less than a micron wide, and approximately 20 nm or less in thickness⁸⁴ (Fig. 16 a-c). Specific contact resistances for Ni and Pd were $\leq 1.1 \times 10^{-4}$ and $\leq 5.9 \times 10^{-4} \Omega \text{ cm}^2$, respectively.

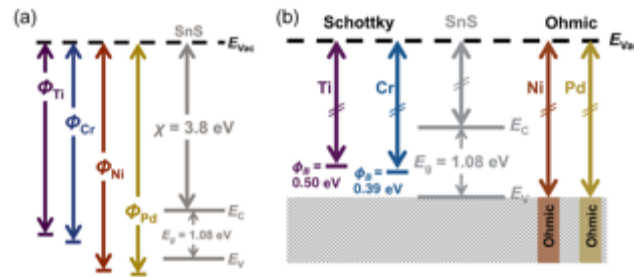


FIG. 15. (a) Schottky–Mott band alignment of metals and (100) SnS. E_{vac} is the vacuum level. χ , E_g , E_c , and E_v are the electron affinity, band gap, conduction band minimum, and valence band maximum of SnS, respectively. (b) Experimental band alignment for metals and SnS nanoribbons. J. R. Hajzus, A. J. Biacchi, S. T. Le, C. A. Richter, A. R. Hight Walker and L. M. Porter, *Nanoscale*, 2018, **10**, 319 - Reproduced by permission of The Royal Society of Chemistry.

This is the author's peer reviewed, accepted manuscript. However, the online version of record will be different from this version once it has been copyedited and typeset.
PLEASE CITE THIS ARTICLE AS DOI: 10.1116/1.5144502

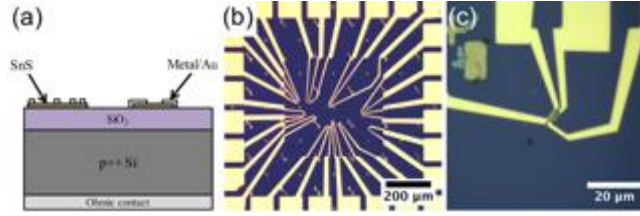


FIG. 16: (a) Cross-sectional schematic of example contact test structures to SnS nanoribbons. (b) Optical microscope image of a sample with many contact test structures, patterned using e-beam lithography and (c) a higher magnification image of a single nanoribbon with four contacts for TLM measurement. J. R. Hajzus, A. J. Biacchi, S. T. Le, C. A. Richter, A. R. Hight Walker and L. M. Porter, *Nanoscale*, 2018, **10**, 319 - Reproduced by permission of The Royal Society of Chemistry.

In contrast, contacts to electron-beam-evaporated, p-type nanocrystalline α -SnS thin films (Fig. 17) did not display the range of electrical behavior observed for contacts to the (100) p-type SnS nanocrystals.⁸⁵ Based on the reported electron affinity = 3.8 eV for (100) α -SnS⁸⁰ and a bandgap of 1.1 eV, one would predict that metals with work functions ~ 5 eV or higher would be ohmic and those with lower work functions would be rectifying. Furthermore, additional crystallographic surfaces exposed in nanocrystalline SnS thin films have reported electron affinities even greater than that of the (100) surface.⁸⁰ However, all of the contacts (Ti/Au, Ru/Au, Ni/Au, and Au) were ohmic in the as-deposited condition, despite the moderate hole concentration ($\sim 5 \times 10^{15} \text{ cm}^{-3}$) of the SnS films.⁸⁵ The average specific contact resistances decreased with increasing metal work function, suggesting a work function dependent Φ_b and indicating at least partial adherence to Schottky-Mott theory.

This is the author's peer reviewed, accepted manuscript. However, the online version of record will be different from this version once it has been copyedited and typeset.
PLEASE CITE THIS ARTICLE AS DOI: 10.1116/1.5144502

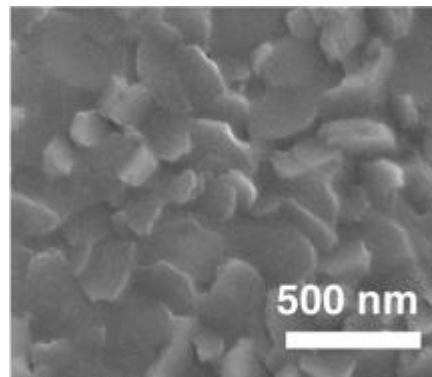


Fig. 17: SEM image of an electron-beam evaporated, nanocrystalline SnS film on a Si substrate. The deposition temperature was 300 °C and post-deposition annealing was conducted at 300 °C for 1 h in high vacuum. Reprinted with permission from J. R. Hajzus, *et al.*, *J. Vac. Sci. Technol., A* **37**, 061504 (2019). Copyright 2019, American Vacuum Society.

In the literature, there is more variability in the electrical behavior of contacts to SnS polycrystalline films, whereas some studies report ohmic behavior for low work function metals⁸⁶⁻⁸⁹ and others report Schottky behavior.^{90, 91} This variability of results among different studies is likely due to the variability in properties (*e. g.* stoichiometry, surface morphology, carrier concentration) of SnS thin films, which have been deposited by a multitude of techniques (*e. g.* electrochemical deposition, thermal evaporation, atomic layer deposition). Furthermore, SnS is known to form a thin oxide layer at its surface⁹² and may be sensitive to differences in surface preparation methods (*e. g.* immersion in ethanol,⁹³ dip in dilute HF,⁸¹ UV-ozone treatment followed by dilute (NH₄)₂S rinse,⁹⁴ O₂ plasma followed by dilute HF dip,⁸⁵ or no reported surface preparation). In the case of our study, we attribute the ohmic behavior of low work function metals on SnS thin films to defect-assisted carrier transport across a non-uniform, nanocrystalline interface.

In addition to high contact resistivity, instability of contacts to SnS can be detrimental to device performance and reliability, particularly for devices, such as thermoelectrics, operating at elevated temperatures.⁶³ Several studies have investigated thermal stability of contacts to SnS. Devika *et al.* found that In and Sn contacts to nanocrystalline SnS thin films were ohmic as deposited. However, contact resistance increased after annealing for 1 min in N₂ between 300 °C - 500 °C, which are temperatures above the melting points of the contact metals.⁸⁸ For the same annealing conditions, Ag, which forms Schottky contacts on SnS crystals⁸² and thin films,⁹¹ developed more linear I-V characteristics and lower contact resistance values.⁸⁸ This result contrasts with other reports that found non-reproducible behavior for Ag contacts to SnS prior to⁸⁶ and after annealing.⁹¹ Notably, Ag is a p-type dopant for SnS,⁹⁵ and diffusion of Ag atoms into SnS could impact properties of the SnS film.

Interfacial reactions and interdiffusion at the metal/SnS interface can have either favorable or detrimental effects on contact behavior. For example, the contact resistance of Pd contacts on SnS thin films decreased after annealing in Ar at 300 °C and 400 °C, whereas annealing at 500 °C degraded the contacts.⁹⁴ Thermodynamic calculations predict Pd contacts are reactive with SnS and interdiffusion at the SnS-Pd contact interface was observed after annealing.⁹⁴ Similarly, certain annealing conditions have been reported to reduce the large as-deposited contact resistance of Ti⁸⁹ and Ti/Au⁹³ contacts to SnS, however higher annealing temperatures were found to destroy the Ti/Au surface morphology.⁹³ In our experiments, the electrical behavior of Ti/Au and Ni/Au contacts to SnS thin films degraded after annealing at 350 °C in Ar.⁸⁵

Au contacts showed greater stability with no significant change in specific contact resistance upon annealing between 300 °C - 500 °C in Ar for 5 min.^{85, 94} Au is not expected to react with SnS based on thermodynamic predictions, and significant intermixing at the Au-SnS interface was not observed.⁹⁴ In contrast, annealing Au/SnS back contact structures in H₂S at 400 °C for 1 hr resulted in an increase in Au contact resistivity,⁸⁹ suggesting the longer annealing time, different annealing ambient, difference in interface geometry, and/or difference in SnS film characteristics permitted diffusion at the interface. Of all contact metals we investigated on SnS thin films, the lowest contact resistivity ($1.9 \times 10^{-3} \Omega \text{ cm}^2$) occurred for Ru/Au contacts annealed at 350 °C in Ar for 5 min.⁸⁵

In summary, the behavior of unannealed contacts to α -SnS appears to be dependent upon the properties of the SnS material itself in addition to the contact metal. Schottky barrier heights of metals on near-ideal (100) surfaces of α -SnS crystals are very close to that predicted by Schottky Mott model, suggesting a lack of Fermi-level pinning for this surface. In contrast, contacts to polycrystalline α -SnS thin films are typically ohmic regardless of metal work function. As-deposited contact resistivities of many metals on polycrystalline SnS films exhibit a decreasing trend with increasing in metal work function, suggesting some dependence of Schottky barrier height on metal work function for polycrystalline SnS films, and that high work function metals should be considered to form low resistance ohmic contacts to SnS films. Certain annealing conditions have been shown to lower the contact resistance of metals such as Pd,⁹⁴ Ru,⁸⁵ Al,⁸⁸ Mo,⁸⁹ Ti^{89, 93} and Ag⁸⁸. However, annealing at high temperatures or for long durations may result in an increase in contact resistance or deterioration of the contact for

certain metals including Pd,⁹⁴ Ti,^{85, 93} Ni,⁸⁵ Al,⁸⁸ Au,⁸⁹ Sn,⁸⁸ and In.⁸⁸ For this reason, the identification of a low resistivity contact that is stable over a range of operating conditions or the development of a diffusion barrier may be beneficial for SnS-based devices.

VI. SUMMARY AND CONCLUSIONS

This paper presents a perspective from our research on metal contacts to four different semiconductors: β -Ga₂O₃, SiC, nanocrystalline diamond, and SnS. It emphasizes published results of Schottky barrier height measurements and factors, such as metal work function, that appear to determine Φ_b . The same factors can also determine whether a particular metal-semiconductor is ohmic or rectifying.

The Schottky-Mott relationship predicts the ideal case in which Φ_b for a particular semiconductor depends directly (and only) on the work function of the metal contact, whereas the index of interface behavior, S , quantifies the actual dependence in practice. The results presented herein indicate that Φ_b is strongly affected by the nature (e.g., surface plane/orientation, cleanliness, defect types/density) of the semiconductor surface (or near surface). In fact, when placed in context of Kurtin, McGill and Mead's seminal paper,⁵ which reports highly covalently-bonded semiconductors as having complete Fermi level pinning ($S \sim 0$) and highly ionically-bonded semiconductors as being completely unpinned ($S = 1$), the results in the present paper indicate that the covalent-vs.-ionic semiconductor distinction is not necessarily universal or absolute. An example is the (100) SnS nanoribbon surface, which followed predictions from Schottky-Mott theory and appears to behave ideally. $S \sim 1$ for (100) SnS nanoribbons, even though SnS's degree of ionicity is slightly less than that of SiC ($S \sim 0.4-0.5$). We believe that this

result may be associated with the fact that SnS is a layered material (i.e., in principle, no dangling bonds) and that the nanoribbons are single crystalline. In contrast, SnS nanocrystalline thin films did not behave as ideally; all contacts were ohmic regardless of the metal work function. For SnS thin films the contact resistance decreased with increasing metal work function, suggesting some dependence of Φ_b on Φ_m .

Surface contamination and defects can also have major effects on the interfacial properties. The difficulty to completely clean the SiC surface may limit contact properties. Φ_b inhomogeneities and device reliability issues have been tied to specific defects in SiC. NCD is inherently inhomogeneous, in essence a composite material: its properties are a combination of the properties of the nanocrystalline diamond grains and the properties of the grain boundaries. The latter dominate the electrically conductive properties of NCD films and likely contribute to the different behavior of contacts to NCD vs. conventional diamond films. Interestingly, although NCD films are by nature highly defective and bonding within diamond grains is covalent, Φ_b showed a significant dependence on the metal work functions ($S \sim 1/3$). The results of Schottky contacts to β -Ga₂O₃ have been dependent on the surface plane. To date (100) and (010) β -Ga₂O₃ surface have shown more 'ideal' metal-semiconductor properties than those on the (-201) β -Ga₂O₃ surface. SiC is another semiconductor that has shown significant differences for different surfaces: e.g., metals on C-face SiC tend to have higher Φ_b 's than the same metals on Si-face SiC.

Ohmic contacts to all of these semiconductors have been demonstrated. Ohmic contacts tend to form readily to NCD and nanocrystalline SnS films, whereas few metals have been demonstrated as ohmic contacts to Ga₂O₃. Although progress has been made to

enhance thermal stability of metal-semiconductor contacts, improvements are needed to realize the full potential of semiconductors like Ga₂O₃ and SiC that are being developed for devices for extreme operating conditions.

ACKNOWLEDGMENTS

Published results from our group would not have been possible without the contributions from many former and current students and colleagues. This work is supported by the Air Force Office of Scientific Research under award number FA9550-18-1-0387.

- ¹N. F. Mott, Proc. Cambr. Philos. Soc. **34**, 538 (1938).
- ²J. Bardeen, Phys. Rev. **71**, 717 (1947).
- ³W. Mönch, Appl. Surf. Sci. **41/42**, 128 (1989).
- ⁴W. Mönch, Rep. Prog. Phys. **53**, 221 (1990).
- ⁵S. Kurtin, T. C. McGill and C. A. Mead, Phys. Rev. Lett. **22**, 1433 (1969).
- ⁶H. Y. Playford, A. C. Hannon, E. R. Barney and R. I. Walton, Chem. Eur. J. **19**, 2803 (2013).
- ⁷M. Zinkevich and F. Aldinger, J. Am. Ceram. Soc. **87**, 683 (2004).
- ⁸M. Higashiwaki, K. Sasaki, A. Kuramata, T. Masui and S. Yamakoshi, Phys. Status Solidi A **211**, 21 (2014).
- ⁹S. J. Pearton, J. Yang, P. H. Cary IV, F. Ren, J. Kim, M. J. Tadjer and M. A. Mastro, Appl. Phys. Rev. **5**, 011301 (2018).
- ¹⁰L. A. M. Lyle, L. Jiang, K. K. Das and L. M. Porter, in *Gallium Oxide – Technology, Devices and Applications*, edited by S. J. Pearton, F. Ren and M. A. Mastro (Elsevier, 2019), pp. 231-262.
- ¹¹C. Hou, R. M. Gazoni, R. J. Reeves and M. W. Allen, Appl. Phys. Lett. **114**, 033502 (2019).
- ¹²T. C. Lovejoy, R. Chen, X. Zheng, E. G. Villora, K. Shimamura, H. Yoshikawa, Y. Yamashita, S. Ueda, K. Kobayashi, S. T. Dunham, F. S. Ohuchi and M. A. Olmstead, Appl. Phys. Lett. **100**, 181602 (2012).



This is the author's peer reviewed, accepted manuscript. However, the online version of record will be different from this version once it has been copyedited and typeset.
PLEASE CITE THIS ARTICLE AS DOI: 10.1116/1.5144502

- ¹³A. Navarro-Quezada, Z. Galazka, S. Alamé, D. Skuridina, P. Vogt and N. Esser, *Appl. Surf. Sci.* **349**, 368 (2015).
- ¹⁴P. D. C. King, T. D. Veal, D. J. Payne, A. Bourlange, R. G. Egdell and C. F. McConville, *Phys. Rev. Lett.* **101**, 116808 (2008).
- ¹⁵R. Suzuki, S. Nakagomi, Y. Kokubun, N. Arai and S. Ohira, *Appl. Phys. Lett.* **94**, 222102 (2009).
- ¹⁶A. Jayawardena, A. C. Ahyi and S. Dhar, *Semicond. Sci. Technol.* **31**, 115002 (2016).
- ¹⁷Y. Yao, R. Gangireddy, J. Kim, K. Das, R. F. Davis and L. M. Porter, *J. Vac. Sci. Technol. B* **35**, 03D113 (2017).
- ¹⁸E. Farzana, Z. Zhang, P. K. Paul, A. R. Arehart and S. A. Ringel, *Appl. Phys. Lett.* **110**, 202102 (2017).
- ¹⁹K. Jiang, L. A. M. Lyle, E. V. Favela, D. Moody, T. Lin, K. K. Das, A. Popp, Z. Galazka, G. Wagner and L. M. Porter, *ECS Transactions* **92**, 71 (2019).
- ²⁰Y. Yao, R. F. Davis and L. M. Porter, *J. Electron. Mater.* **46**, 2053 (2016).
- ²¹H. K. Kim, K. K. Kim, S. J. Park, T. Y. Seong and I. Adesida, *J. Appl. Phys.* **94**, 4225 (2003).
- ²²L. J. Brillson, H. L. Mosbacker and M. J. Hetzer, *Appl. Phys. Lett.* **90**, 102116 (2007).
- ²³M.-H. Lee and R. L. Peterson, *APL Mater.* **7**, 022524 (2019).
- ²⁴K. Sasaki, M. Higashiwaki, A. Kuramata, T. Masui and Y. Shigenobu, *Appl. Phys. Express* **6**, 086502 (2013).
- ²⁵J. Shi, X. Xia, H. Liang, Q. Abbas, J. Liu, H. Zhang and Y. Liu, *J. Mater. Sci.* **30**, 3860 (2019).
- ²⁶N. Kaminski, S. Rugen and F. Hoffmann, presented at the IEEE International Reliability Physics Symposium, 2019 (unpublished).
- ²⁷T. Kimoto, H. Niwa, N. Kaji, T. Kobayashi, Y. Zhao, S. Mori and M. Aketa, presented at the IEEE Int. Electron Devices Meet. (IEDM 2017), 2017 (unpublished).
- ²⁸P. J. Wellmann, *Journal of Inorganic and General Chemistry* **643**, 1312 (2017).
- ²⁹L. M. Porter, R. F. Davis, J. S. Bow, M. J. Kim, R. W. Carpenter and R. C. Glass, *J. Mater. Res.* **10**, 668 (1995).
- ³⁰A. J. van Bommel, J. E. Crombeen and A. van Tooren, *Surface Science* **48**, 463 (1975).

- ³¹J. R. Waldrop, R. W. Grant, Y. C. Wang and R. F. Davis, *J. Appl. Phys.* **72**, 4757 (1992).
- ³²J. R. Waldrop and R. W. Grant, *Appl. Phys. Lett.* **62**, 2685 (1993).
- ³³L. M. Porter and R. F. Davis, *Mater. Sci. Eng. B* **34**, 83 (1995).
- ³⁴L. M. Porter, R. F. Davis, J. S. Bow, M. J. Kim and R. W. Carpenter, *J. Mater. Res.* **10**, 26 (1995).
- ³⁵L. M. Porter, R. F. Davis, J. S. Bow, M. J. Kim and R. W. Carpenter, *J. Mater. Res.*, 2336 (1995).
- ³⁶L. M. Porter, R. F. Davis, J. S. Bow, M. J. Kim and R. W. Carpenter, *J. Mater. Res.* **10**, 2336 (1995).
- ³⁷D. J. Ewing, L. M. Porter, Q. Wahab, X. Ma, T. S. Sudharshan, S. Tumakha, M. Gao and L. J. Brillson, *J. Appl. Phys.* **101**, 114514 (2007).
- ³⁸S. Tumakha, D. J. Ewing, L. M. Porter, Q. Wahab, X. Ma, T. S. Sudarshan and L. J. Brillson, *Appl. Phys. Lett.* **87**, 242106 (2005).
- ³⁹D. Defives, O. Noblanc, C. Dua, C. Brylinski, M. Barthula and F. Meyer, *Mater. Sci. Eng. B* **61/62**, 395 (1999).
- ⁴⁰B. J. Skromme, E. Luckowski, K. Moore, M. Bharnagar, C. E. Weitzel, T. Gehoski and D. Ganser, *J. Electron. Mater.* **29**, 376 (2000).
- ⁴¹F. Roccaforte, P. Fiorenza, G. Greco, R. Lo Nigro, F. Giannazzo, F. Iucolano and M. Saggio, *Microelectronic Engineering* **187-188**, 66 (2018).
- ⁴²J. Crofton, L. M. Porter and J. R. Williams, *phys. stat. sol. (b)* **202**, 581 (1997).
- ⁴³R. Okojie and D. Lukco, *J. Appl. Phys.* **120**, 215301 (2016).
- ⁴⁴Y. Zhang, T. Guo, X. Tang, J. Yang, Y. He and Y. Zhang, *J. Alloys Compd.* **731**, 1267 (2018).
- ⁴⁵K. C. Kragh-Buetow, R. Okojie, D. Lukco and S. E. Mohny, *Semicond. Sci. Technol.* **30**, 105019 (2015).
- ⁴⁶O. A. Williams, *Diamond and Related Materials* **20**, 621 (2011).
- ⁴⁷P. Achatz, J. A. Garrido, M. Stutzmann, O. A. Williams, D. M. Gruen, A. Kromka and Steinmüller, *Appl. Phys. Lett.* **88**, 101908 (2006).
- ⁴⁸P. Kulkarni, L. M. Porter, F. A. M. Koeck, Y.-J. Tang and R. J. Nemanich, *J. Appl. Phys.* **103**, 084905 (2008).

- ⁴⁹Q. Hu, M. Hirai, K. J. Rakesh and A. Kumar, *J. Phys. D* **42**, 025301 (2009).
- ⁵⁰H. Gomez, A. Kumar and S. Jeedigunta, *International Journal of Nanomanufacturing* **4**, 317 (2009).
- ⁵¹J. E. Gerbi, O. Auciello, J. Birrell, D. M. Gruen, B. W. Alphenaar and J. A. Carlisle, *Appl. Phys. Lett.* **83**, 2001 (2003).
- ⁵²M. Vojs, A. Kromka, T. Izak, J. Skriniarova, I. Novotny, P. Valent, M. Michalka, T. Kovacik and M. Vesely, *Journal of Physics: Conference Series* **100**, 052097 (2008).
- ⁵³C. R. Lin, D. H. Wei, M. K. BenDao, W. E. Chen and T. Y. Liu, *International Journal of Photoenergy* **2014**, 492152 (2014).
- ⁵⁴C.-W. Liu, J.-A. Lee, Y.-T. A. Sun, M.-K. BenDao and C.-R. Lin, *Appl. Surf. Sci.* **455**, 581 (2018).
- ⁵⁵M. J. Tadjer, T. J. Anderson, K. D. Hobart, T. I. Feygelson, J. E. Butler and F. J. Kub, *Materials Science Forum* **645-648**, 733 (2010).
- ⁵⁶S. Jeedigunta, Z. Xu, M. Hirai, P. Spagnol and A. Kumar, *Diamond and Related Materials* **17**, 1994 (2008).
- ⁵⁷C. Pietzka, A. Denisenko, M. Dipalo and E. Kohn, *Diamond and Related Materials* **19**, 56 (2010).
- ⁵⁸J. M. Skelton, L. A. Burton, F. Oba and A. Walsh, *J. Phys. Chem. C* **121**, 6446 (2017).
- ⁵⁹J. Vidal, S. Lany, M. d'Avezac, A. Zunger, A. Zakutayev, J. Francis and J. Tate, *Appl. Phys. Lett.* **100** 032104 (2012).
- ⁶⁰L. A. Burton, D. Colombara, R. D. Abellon, F. C. Grozema, L. M. Peter, T. J. Savenije, G. Dennler and A. Walsh, *Chem. Mater.* **25**, 4908 (2013).
- ⁶¹R. E. Banai, M. W. Horn and J. R. S. Brownson, *Sol. Energy Mater. Sol. Cells* **150**, 112 (2016).
- ⁶²G. A. Tritsarlis, B. D. Malone and E. Kaxiras, *J. Appl. Phys.* **113** 233507 (2013).
- ⁶³W. K. He, D. Y. Wang, H. J. Wu, Y. Xiao, Y. Zhang, D. S. He, Y. Feng, Y. J. Hao, J. F. Dong, R. Chetty, L. J. Hao, D. F. Chen, J. F. Qin, Q. Yang, X. Li, J. M. Song, Y. C. Zhu, W. Xu, C. L. Niu, G. T. Wang, C. Liu, M. Ohta, S. J. Pennycook, J. Q. He, J. F. Li and L. D. Zhao, *Science* **365**, 1418 (2019).

- ⁶⁴T. F. Zhou, W. K. Pang, C. F. Zhang, J. P. Yang, Z. X. Chen, H. K. Liu and Z. P. Guo, *ACS Nano* **8**, 8323 (2014).
- ⁶⁵X. Zhou, L. Gan, Q. Zhang, X. Xiong, H. Q. Li, Z. Q. Zhong, J. B. Han and T. Y. Zhai, *J. Mater. Chem. C* **4**, 2111 (2016).
- ⁶⁶I. Lefebvre, M. A. Szymanski, J. Olivier-Fourcade and J. C. Jumas, *Phys. Rev. B* **58**, 1896 (1998).
- ⁶⁷L. C. Gomes and A. Carvalho, *Phys. Rev. B* **92**, 085406 (2015).
- ⁶⁸A. K. Singh and R. G. Hennig, *Appl. Phys. Lett.* **105** 042103 (2014).
- ⁶⁹L. Huang, F. G. Wu and J. B. Li, *J. Chem. Phys.* **144**, 114708 (2016).
- ⁷⁰C. Xin, J. X. Zheng, Y. T. Su, S. K. Li, B. K. Zhang, Y. C. Feng and F. Pan, *J. Phys. Chem. C* **120**, 22663 (2016).
- ⁷¹C. Chowdhury, S. Karmakar and A. Datta, *J. Phys. Chem. C* **121**, 7615 (2017).
- ⁷²R. Fei, W. Li, J. Li and L. Yang, *Appl. Phys. Lett.* **107**, 173104 (2015).
- ⁷³M. H. Wu and X. C. Zeng, *Nano Lett.* **16**, 3236 (2016).
- ⁷⁴J. R. Brent, D. J. Lewis, T. Lorenz, E. A. Lewis, N. Savjani, S. J. Haigh, G. Seifert, B. Derby and P. O'Brien, *J. Am. Chem. Soc.* **137**, 12689 (2015).
- ⁷⁵Y. F. Sun, Z. H. Sun, S. Gao, H. Cheng, Q. H. Liu, F. C. Lei, S. Q. Wei and Y. Xie, *Adv. Energy Mater.* **4** 1300611 (2014).
- ⁷⁶N. Higashitarumizu, H. Kawamoto, M. Nakamura, K. Shimamura, N. Ohashi, K. Ueno and K. Nagashio, *Nanoscale* **10**, 22474 (2018).
- ⁷⁷W. Albers, H. J. Vink, C. Haas and J. D. Wasscher, *J. Appl. Phys.* **32**, 2220 (1961).
- ⁷⁸R. E. Banai, L. A. Burton, S. G. Choi, F. Hofherr, T. Sorgenfrei, A. Walsh, B. To, A. Croll and J. R. S. Brownson, *J. Appl. Phys.* **116** 013511 (2014).
- ⁷⁹G. A. Tritsarlis, B. D. Malone and E. Kaxiras, *J. Appl. Phys.* **115** 173702 (2014).
- ⁸⁰V. Stevanovic, K. Hartman, R. Jaramillo, S. Ramanathan, T. Buonassisi and P. Graf, *Appl. Phys. Lett.* **104** 211603 (2014).
- ⁸¹J. R. Hajzus, A. J. Biacchi, S. T. Le, C. A. Richter, A. R. H. Walker and L. M. Porter, *Nanoscale* **10**, 319 (2018).
- ⁸²S. Karadeniz, M. Sahin, N. Tugluoglu and H. Safak, *Semicond. Sci. Technol.* **19**, 1098 (2004).



- ⁸³S. Sucharitakul, U. R. Kumar, R. Sankar, F. C. Chou, Y. T. Chen, C. H. Wang, C. He, R. He and X. P. A. Gao, *Nanoscale* **8**, 19050 (2016).
- ⁸⁴A. J. Biacchi, S. T. Le, B. G. Alberding, J. A. Hagmann, S. J. Pookpanratana, E. J. Heilweil, C. A. Richter and A. R. H. Walker, *ACS Nano* **12**, 10045 (2018).
- ⁸⁵J. R. Hajzus and L. M. Porter, *J. Vac. Sci. Technol., A* **37**, 061504 (2019).
- ⁸⁶N. Sato, M. Ichimura, E. Arai and Y. Yamazaki, *Sol. Energy Mater. Sol. Cells* **85**, 153 (2005).
- ⁸⁷N. K. Reddy, M. Devika and K. Gunasekhar, *Thin Solid Films* **558**, 326 (2014).
- ⁸⁸M. Devika, N. K. Reddy, F. Patolsky and K. R. Gunasekhar, *J. Appl. Phys.* **104** 124503 (2008).
- ⁸⁹C. X. Yang, L. Z. Sun, R. E. Brandt, S. B. Kim, X. Z. Zhao, J. Feng, T. Buonassisi and R. G. Gordon, *J. Appl. Phys.* **122** 045303 (2017).
- ⁹⁰N. R. Mathews, *Semicond. Sci. Technol.* **25** 105010 (2010).
- ⁹¹B. Ghosh, M. Das, P. Banerjee and S. Das, *Solid State Sci.* **11**, 461 (2009).
- ⁹²A. de Kergommeaux, J. Faure-Vincent, A. Pron, R. de Bettignies, B. Malaman and P. Reiss, *J. Am. Chem. Soc.* **134**, 11659 (2012).
- ⁹³K. R. Nandanapalli, D. Mudusu and G. K. Reddy, *Mater. Sci. Semicond. Process.* **100**, 192 (2019).
- ⁹⁴R. L. Gurunathan, J. Nasr, J. J. Cordell, R. A. Banai, M. Abraham, K. A. Cooley, M. Horn and S. E. Mohny, *J. Electron. Mater.* **45**, 6300 (2016).
- ⁹⁵Q. Tan, L. D. Zhao, J. F. Li, C. F. Wu, T. R. Wei, Z. B. Xing and M. G. Kanatzidis, *J. Mater. Chem. A* **2**, 17302 (2014).

BIOGRAPHY INFORMATION

Lisa M. Porter is Professor of Materials Science and Engineering at Carnegie Mellon University in Pittsburgh, Pennsylvania, U.S.A. She started at Carnegie Mellon in 1997 as an assistant professor and was promoted to associate professor in 2002 and full professor in 2006. She earned a B.S. and a Ph.D. in Materials Science and Engineering at Cornell University (1989) and N.C. State University (1994), respectively. Her research expertise

pertains to fabrication, processing, and characterization of electronically-functional interfaces and has included dielectric-semiconductor (e.g., SiO₂/SiC) and semiconductor-semiconductor (e.g., InGaN/GaN multi-quantum wells for LEDs) interfaces, with emphasis on metal-semiconductor contacts. In addition to the semiconductors presented in this paper (Ga₂O₃, SiC, nanocrystalline diamond, and SnS), Dr. Porter's research has covered a broad range of (semi)conducting materials such as transparent conductors (e.g., indium-tin-oxide and Ag nanowire/polymer composites), Group-III (Al,Ga,In) nitrides, and the semiconducting polymer polythiophene. Her group currently focuses on gallium oxide and related alloys as a promising new ultra-wide bandgap semiconductor technology for more energy efficient electronics. Some of her awards include the N.C. State MSE Alumni Hall of Fame (2018), the Philbrook Prize in Engineering from CMU (2012), a National Science Foundation Career Award (1999-2004) and a National Swedish Foundation Visiting Professorship (2000-2002). Last year she was honored to present a Plenary Talk at the Taiwan Association for Coatings and Technology Annual Meeting in Taipei, Taiwan.

Dr. Porter is proud of the high level of professional service that she has contributed to the scientific community throughout her career. She holds, and has held, leadership positions in a number of professional organizations. She was especially honored to serve as 2018 President of the American Vacuum Society (AVS). In this role she supported efforts by many dedicated volunteers and staff members to launch the new AVS Quantum Science Journal, to educate and engage the AVS community regarding Reproducibility and Replicability issues, and to prepare a foundation for a new five-year strategic plan for the Society, while doing her best to keep tabs on countless other

important activities and initiatives. Prior to serving as AVS President, she was the Program Chair for the AVS 63rd International Symposium (2016) and Program Chair / Division Chair for the Electronic Materials & Photonics Division (2011/2012). Dr. Porter has been a Committee Member or Invited Co-Organizer of the Electronic Materials Conference continuously since 1999; she served as EMC Secretary from 2017-2019 and was elected Program Chair for EMC 2020 and 2021. She is also an ABET Program Evaluator for materials engineering programs. Dr. Porter feels especially privileged to be able to help educate the next generation of scientists and engineers. Former Ph.D. students from her group hold positions in industry (e.g., Intel, IBM, Seagate, LG, Sensit) and government/national labs (e.g., Sandia, DOE, NRL). She and a former Ph.D. student were also cofounders of a company, SenSevere, LLC, which commercialized chemical sensors for extreme environments. Another former Ph.D. student kindly agreed to participate as a coauthor of this Invited Perspective.

“What would I tell my 16-year-old self?”

Don't let other people define your success. Success is what makes you happy and gives you a sense of pride in helping to make the world a little bit better place.

Jenifer R. Hajzus received her B.S. degree in Physics from Rensselaer Polytechnic Institute in 2012, and M.S. and Ph.D. degrees in Materials Science and Engineering from Carnegie Mellon University in 2014 and 2018, respectively. Her graduate thesis work involved the investigation of metal contacts to SnS and the deposition and

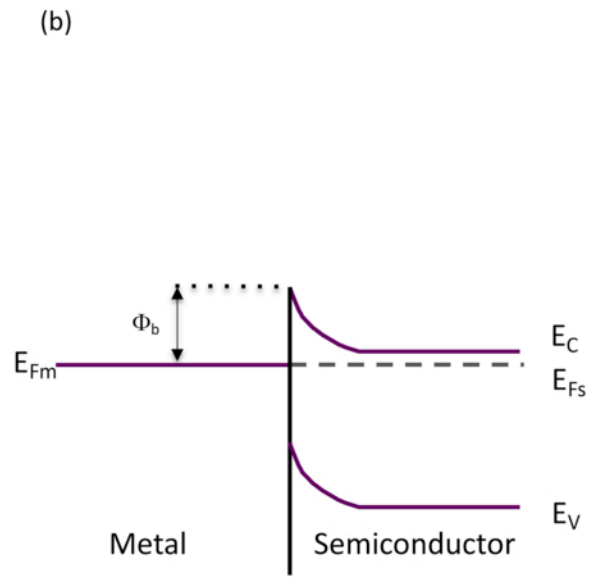
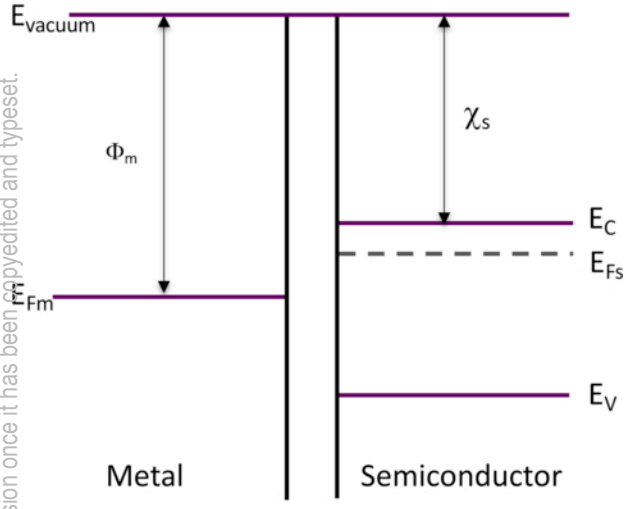


This is the author's peer reviewed, accepted manuscript. However, the online version of record will be different from this version once it has been copyedited and typeset.

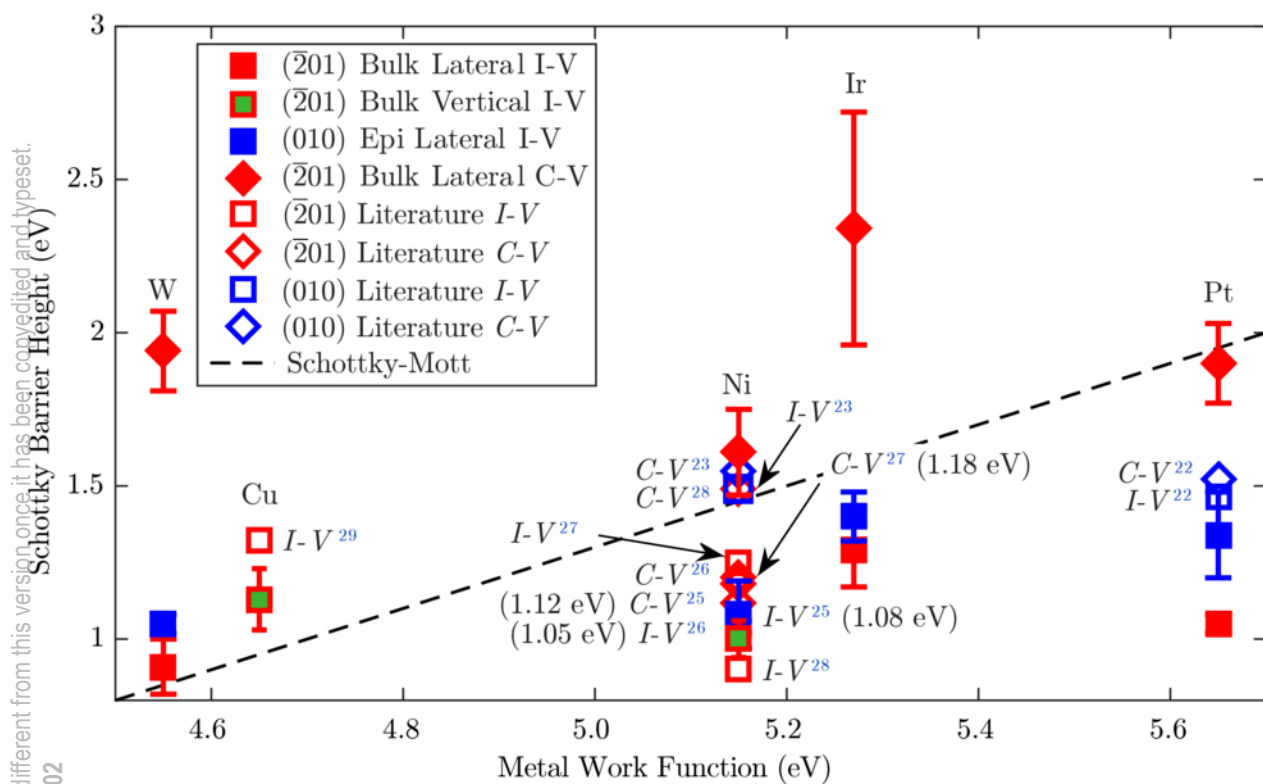
PLEASE CITE THIS ARTICLE AS DOI: 10.1116/1.5144502

characterization of SnS thin films. She is currently an ASEE Postdoctoral Fellow at the U.S. Naval Research Laboratory where her research interests include processing and growth of epitaxial graphene for sensor applications.

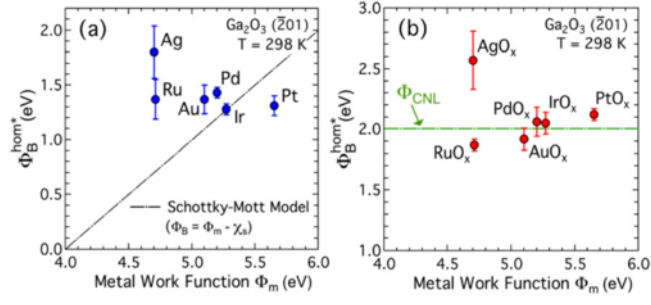
This is the author's peer reviewed, accepted manuscript. However, the online version of record will be different from this version once it has been copyedited and typeset.
PLEASE CITE THIS ARTICLE AS DOI: 10.1116/1.5144502



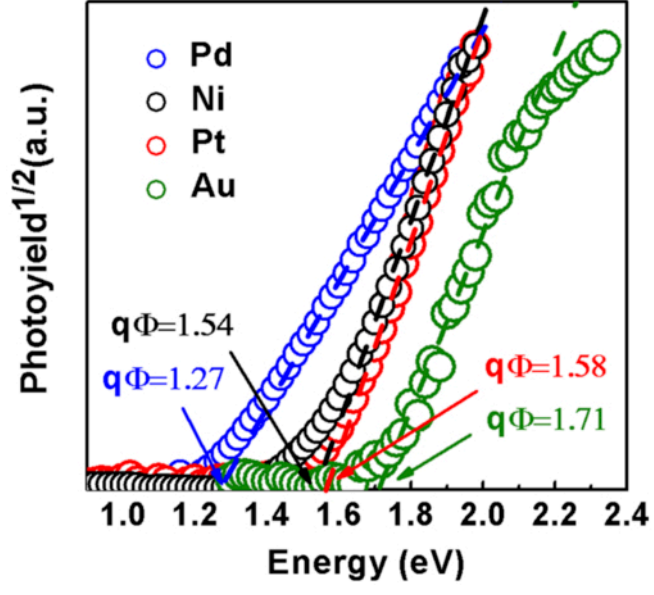
This is the author's peer reviewed, accepted manuscript. However, the online version of record will be different from this version once it has been copyedited and typeset.
PLEASE CITE THIS ARTICLE AS DOI: 10.1116/1.5144502



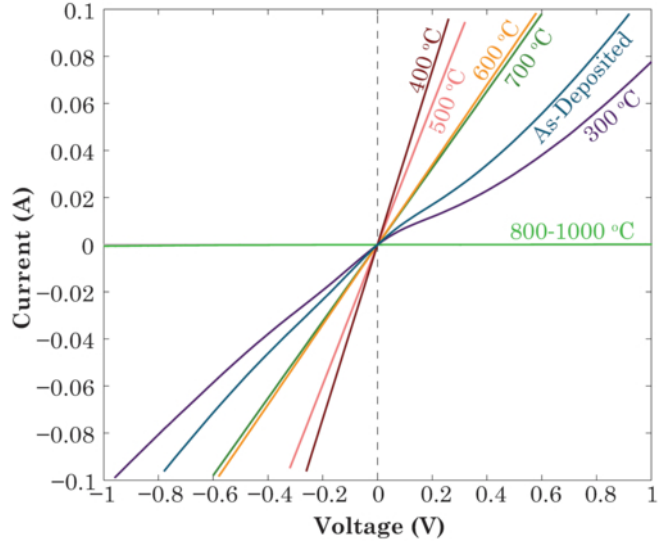
This is the author's peer reviewed, accepted manuscript. However, the online version of record will be different from this version once it has been copyedited and typeset.
PLEASE CITE THIS ARTICLE AS DOI: 10.1116/1.5144502



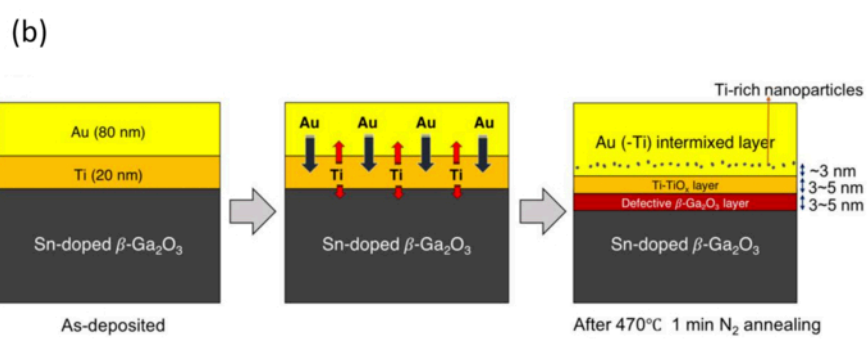
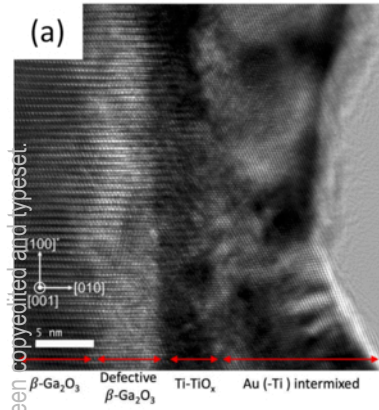
This is the author's peer reviewed, accepted manuscript. However, the online version of record will be different from this version once it has been copyedited and typeset.
PLEASE CITE THIS ARTICLE AS DOI: 10.1116/1.5144502



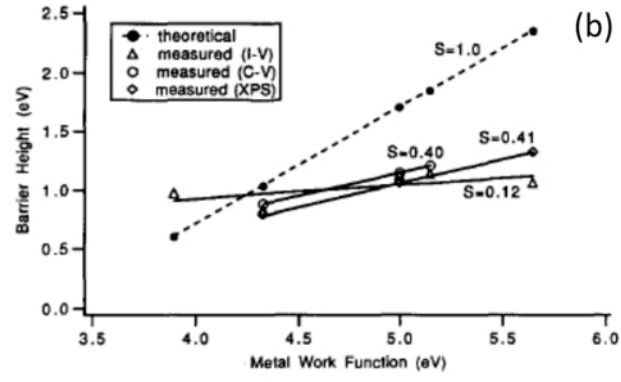
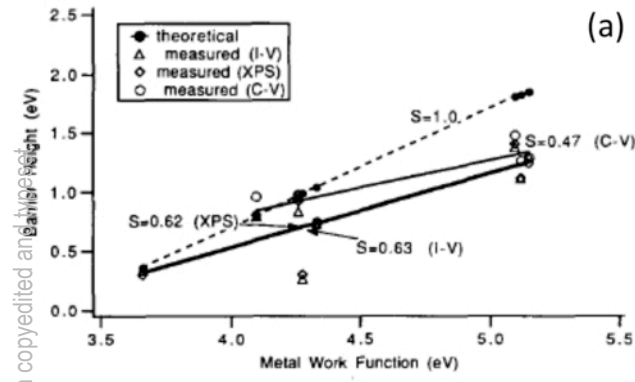
This is the author's peer reviewed, accepted manuscript. However, the online version of record will be different from this version once it has been copyedited and typeset.
PLEASE CITE THIS ARTICLE AS DOI: 10.1116/1.5144502



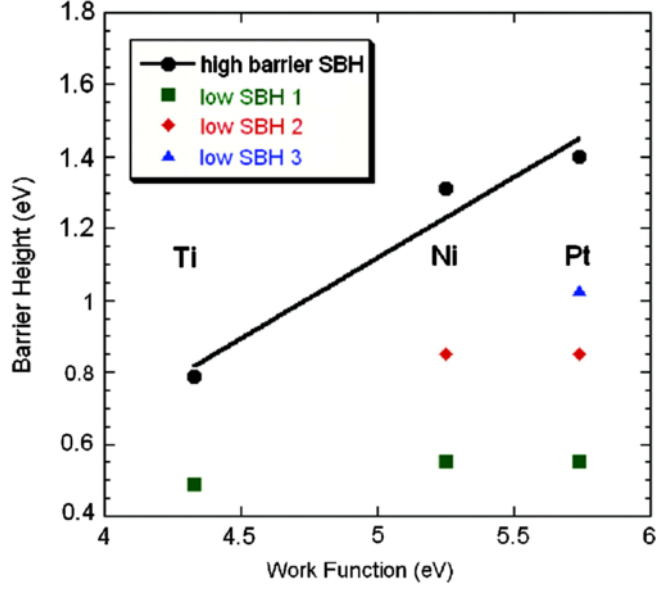
This is the author's peer reviewed, accepted manuscript. However, the online version of record will be different from this version once it has been copyedited and typeset.
PLEASE CITE THIS ARTICLE AS DOI: 10.1116/1.5144502



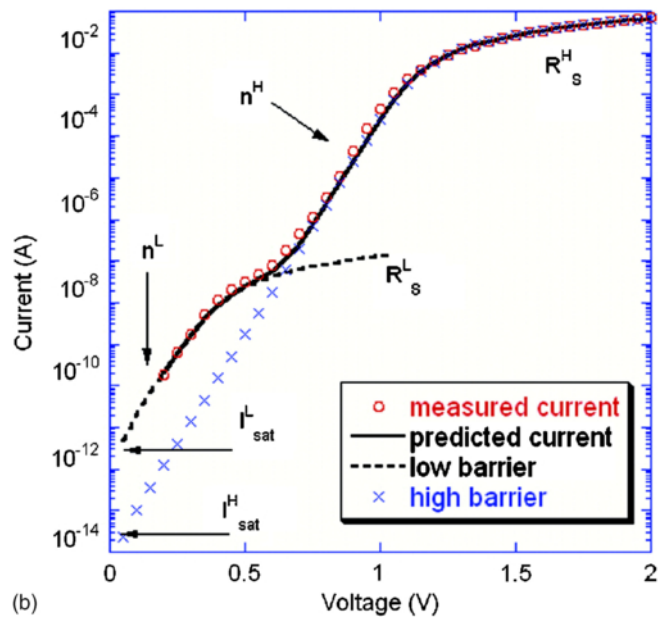
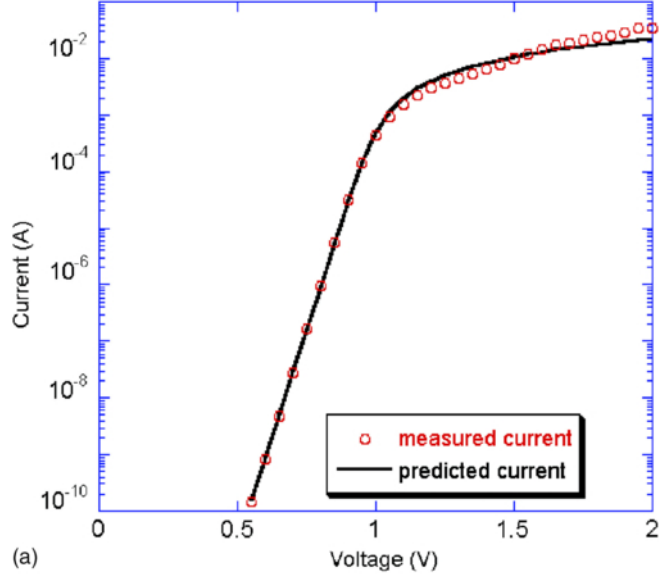
This is the author's peer reviewed, accepted manuscript. However, the online version of record will be different from this version once it has been copyedited and typeset.
PLEASE CITE THIS ARTICLE AS DOI: 10.1116/1.5144502



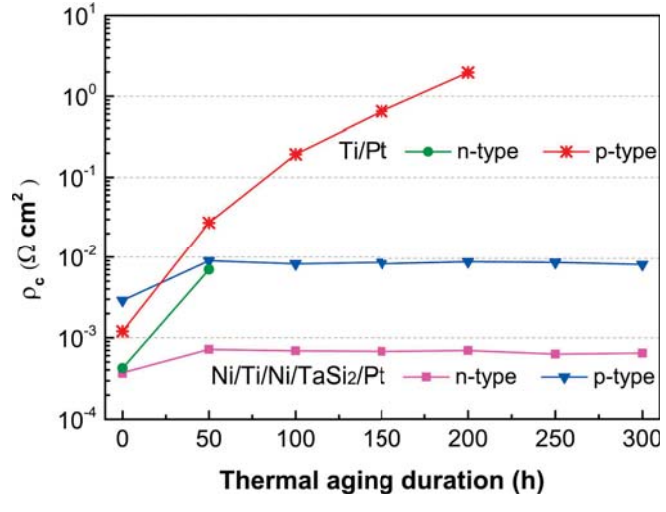
This is the author's peer reviewed, accepted manuscript. However, the online version of record will be different from this version once it has been copyedited and typeset.
PLEASE CITE THIS ARTICLE AS DOI: 10.1116/1.5144502



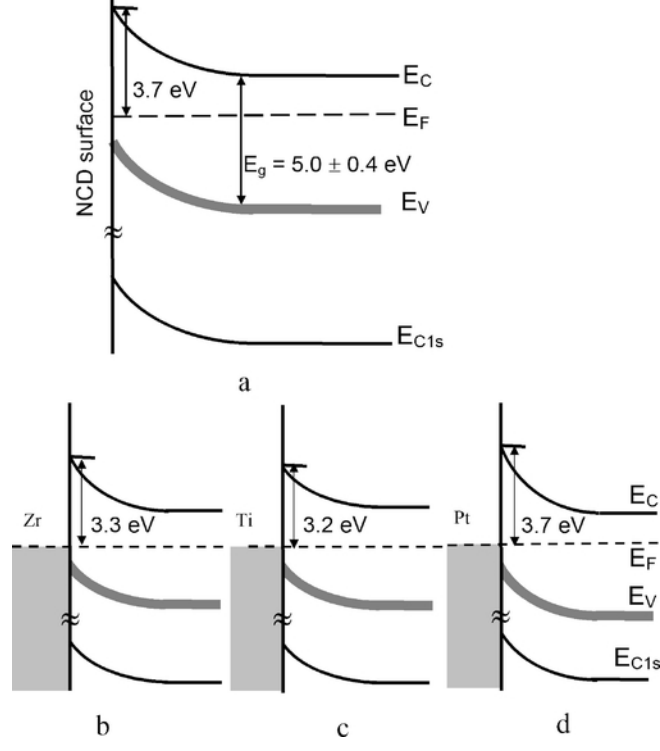
This is the author's peer reviewed, accepted manuscript. However, the online version of record will be different from this version once it has been copyedited and typeset.
PLEASE CITE THIS ARTICLE AS DOI: 10.1116/1.5144502



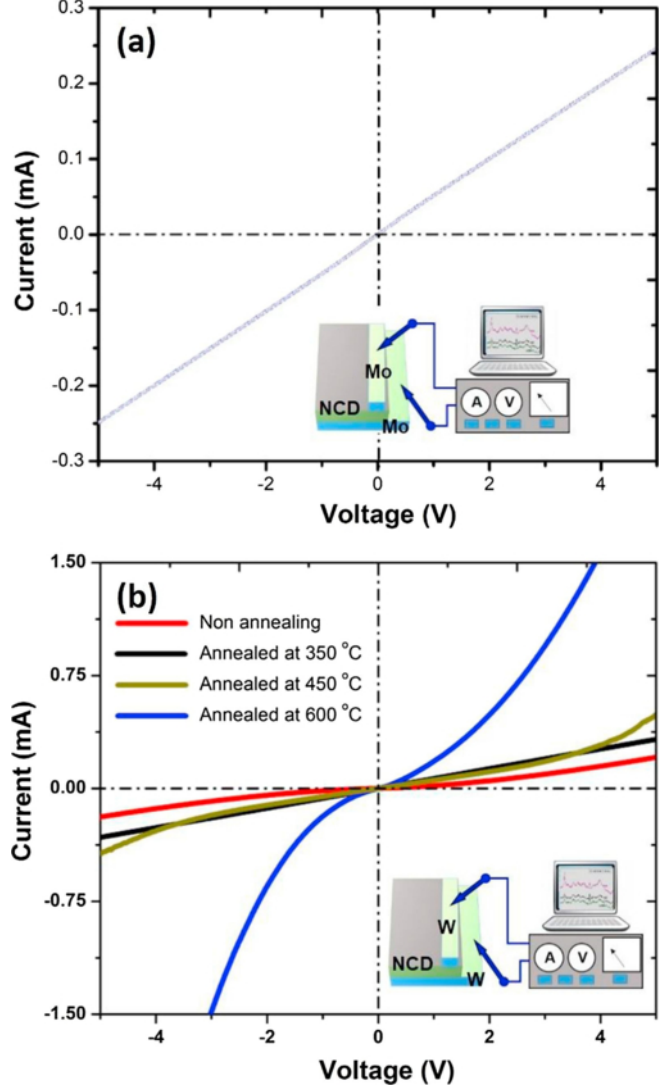
This is the author's peer reviewed, accepted manuscript. However, the online version of record will be different from this version once it has been copyedited and typeset.
PLEASE CITE THIS ARTICLE AS DOI: 10.1116/1.5144502



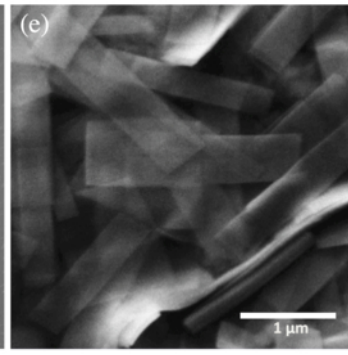
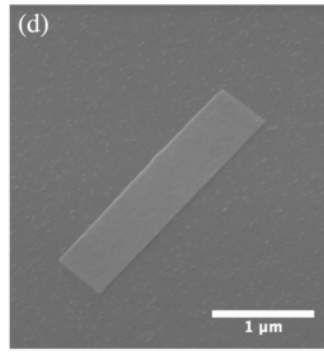
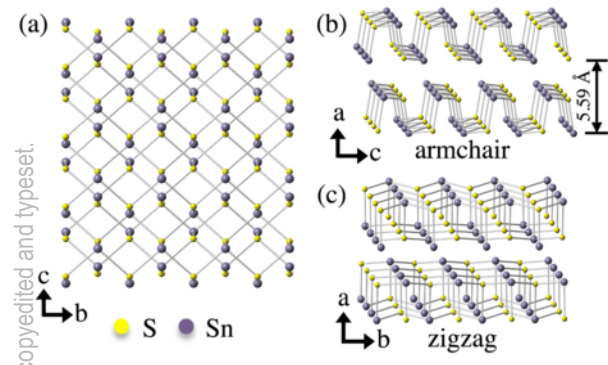
This is the author's peer reviewed, accepted manuscript. However, the online version of record will be different from this version once it has been copyedited and typeset.
PLEASE CITE THIS ARTICLE AS DOI: 10.1116/1.5144502



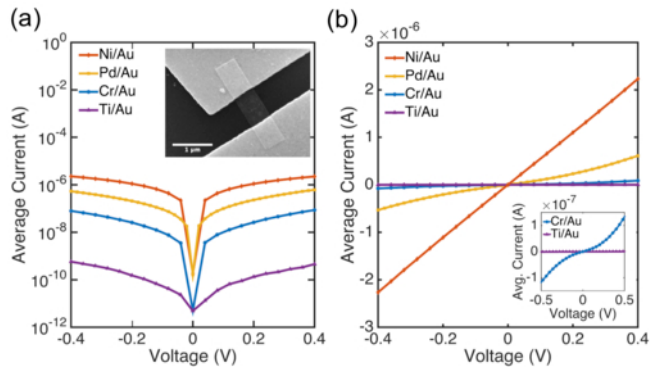
This is the author's peer reviewed, accepted manuscript. However, the online version of record will be different from this version once it has been copyedited and typeset.
PLEASE CITE THIS ARTICLE AS DOI: 10.1116/1.5144502



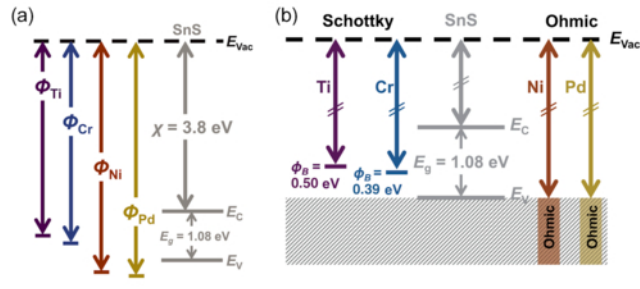
This is the author's peer reviewed, accepted manuscript. However, the online version of record will be different from this version once it has been copyedited and typeset.
PLEASE CITE THIS ARTICLE AS DOI: 10.1116/1.5144502



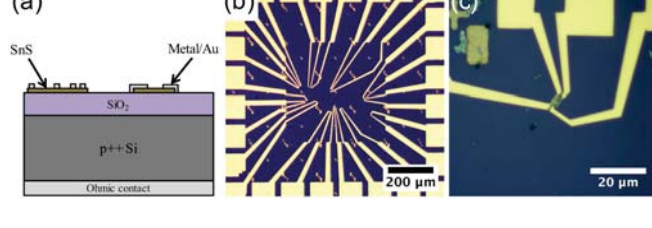
This is the author's peer reviewed, accepted manuscript. However, the online version of record will be different from this version once it has been copyedited and typeset.
PLEASE CITE THIS ARTICLE AS DOI: 10.1116/1.5144502



This is the author's peer reviewed, accepted manuscript. However, the online version of record will be different from this version once it has been copyedited and typeset.
PLEASE CITE THIS ARTICLE AS DOI: 10.1116/1.5144502

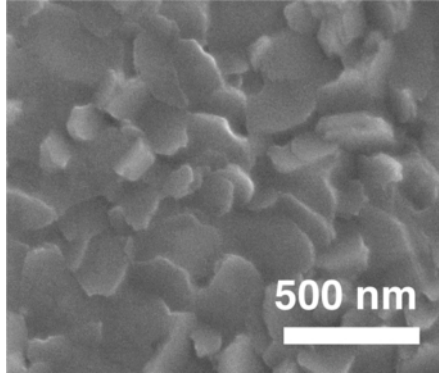


This is the author's peer reviewed, accepted manuscript. However, the online version of record will be different from this version once it has been copyedited and typeset.
PLEASE CITE THIS ARTICLE AS DOI: 10.1116/1.5144502





This is the author's peer reviewed, accepted manuscript. However, the online version of record will be different from this version once it has been copyedited and typeset.
PLEASE CITE THIS ARTICLE AS DOI: 10.1116/1.5144502





This is the author's peer reviewed, accepted manuscript. However, the online version of record will be different from this version once it has been copyedited and typeset.
PLEASE CITE THIS ARTICLE AS DOI: 10.1116/1.5144502





This is the author's peer-reviewed, accepted manuscript. However, the online version of record will be different from this version once it has been copyedited and typeset.
PLEASE CITE THIS ARTICLE AS DOI: 10.1116/1.5144502

